U-Pb and Ar-Ar geochronological data from the Pelagonian basement in Evia (Greece): geodynamic implications for the evolution of Paleotethys

by I. Vavassis[1], A. De Bono[1], G.M. Stampfli[1], D. Giorgis[2], A. Valloton[1], and Y. Amelin[3]

Abstract

High precision U-Pb zircon and $^{40}Ar/^{39}Ar$ mica geochronological data on metagranodiorites, metagranites and mica schists from north and central Evia island (Greece) are presented in this study. U-Pb zircon ages range from 308 to 1912 Ma, and indicate a prolonged magmatic activity in Late Carboniferous. Proterozoic ages represent inherited cores within younger crystals. Muscovite $^{40}Ar/^{39}Ar$ plateau ages of 288 to 297 Ma are interpreted as cooling ages of the magmatic bodies and metamorphic host rocks in upper greenschist to epidote-amphibolite metamorphic conditions. The multistage magmatism had a duration between 308 and 319 Ma but some older intrusions, as well as metamorphic events, cannot be excluded. Geochemical analyses and zircon typology indicate calc-alkaline affinities for the granites of central Evia and alkaline to calc-alkaline characteristics for the metagranodiorites from the northern part of the island. The new data point towards the SE continuation, in Evia and the Cyclades, of a Variscan continental crust already recognised in northern Greece (Pelagonian basement). The Late Carboniferous magmatism is viewed as a result of northward subduction of the Paleotethys under the Eurasian margin.

Keywords: Greece, Variscan, Evia, Pelagonia, zircon and mica dating, Late Carboniferous, Permian, Eocimmerian, Paleotethys.

Introduction

The Internal Hellenides comprise several imbricated tectonic units of which the Pelagonian unit is the largest, affected by two main orogenic events. The first event (the Eo-Hellenic phase) occurred during Late Jurassic-Early Cretaceous time, following the obduction of the Vardar ocean ophiolites (JACOBSHAGEN and ROEDER, 1976). The second event is related to the Alpine orogeny (the Meso-Hellenic phase) and corresponds to the final closure of the ocean during the Late Paleocene to Late Eocene. A characteristic of the Internal Hellenides is the Late Cretaceous transgression sealing the obduction. The upper Cretaceous sequence consists of Cenomanian conglomerates and neritic limestones as well as bauxitic and iron-nickel deposits overlain by pelagic Maastrichtian limestones and Paleocene flysch

(KATSIKATSOS et al., 1986). In contrast, the External Hellenides record only Alpine tectonic events. The Attica-Cyclades Crystalline Belt of the Hellenides contains tectonic units which underwent high pressure / low temperature (HP/LT) metamorphism in the Late Cretaceous to Late Eocene as well as Barrovian metamorphism and intrusion of granitoids during the Late Oligocene and Miocene (ALTHERR et al., 1982; LISTER et al., 1994 and BRÖCKER and FRANZ, 1998; BRÖCKER and ENDERS, 1999). Rare findings of fossils found at Andros (PAPANIKOLAOU, 1978), Paros (PAPANIKOLAOU, 1980), Naxos (NEGRIS, 1915; DÜRR and FLÜGEL, 1979), Tinos (MELIDONIS, 1980) and Samos (PAPANIKOLAOU, 1979) have shown that these sequences are post-Variscan. In an attempt to refine the paleoreconstruction of the Western Tethys from the Early Paleozoic to the Late Mesozoic, the age and origin of the Internal Hel-

[1] Institut de Géologie et Paléontologie, Université de Lausanne, BFSH2, CH-1015 Lausanne, Switzerland.
<gerard.stampfli@igp.unil.ch> <ioannis.vavassis@igp.unil.ch>
[2] Institut de Minéralogie et Géochimie, Université de Lausanne, BFSH2, CH-1015 Lausanne, Switzerland.
[3] Department of Geology, Royal Ontario Museum, Toronto, Canada M5S 2C6.
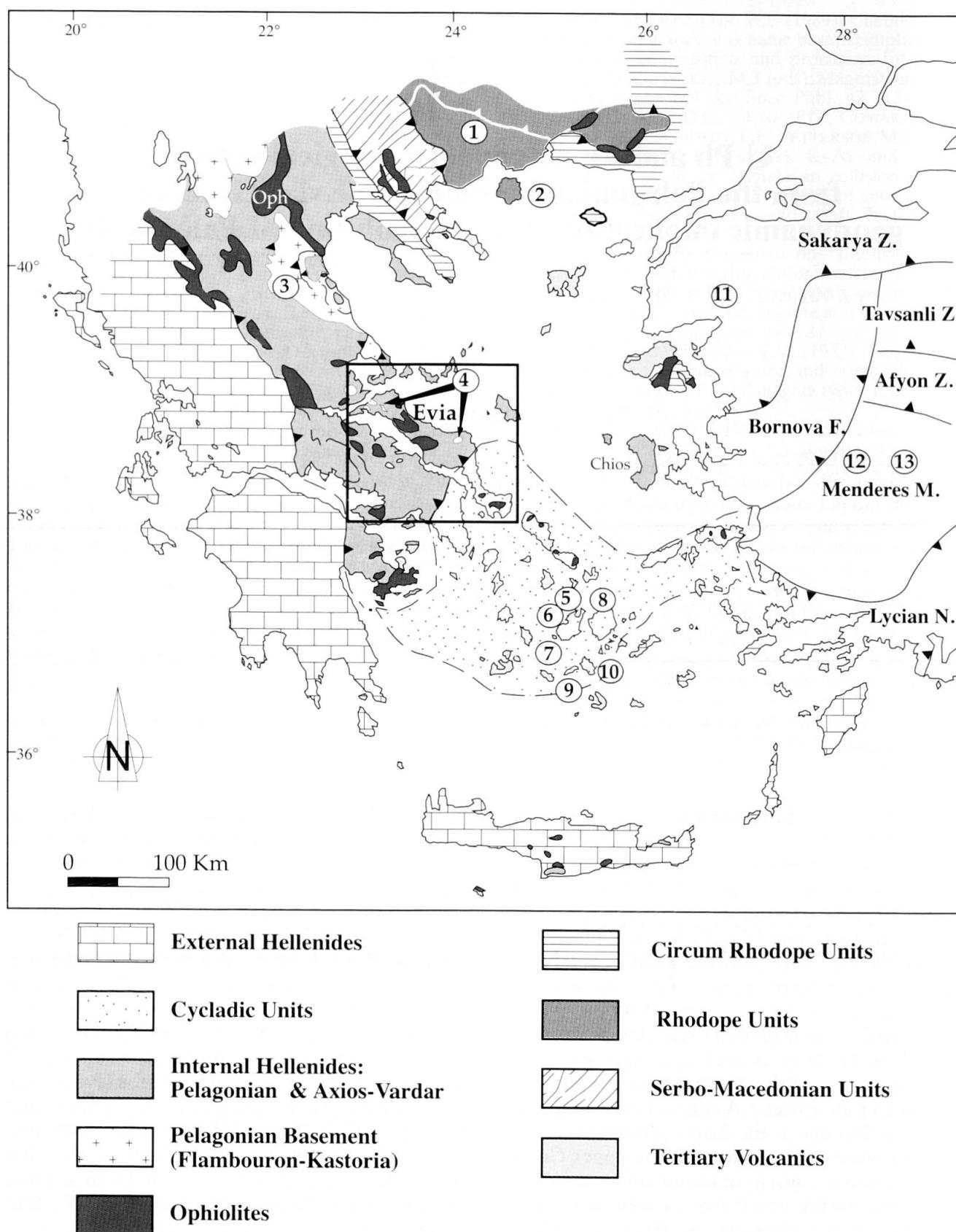
Fig. 1   Main tectonic domains in Greece and Western Turkey; numbers correspond to the geochronological data presented in table 2. (Modified from PAPANIKOLAOU, 1989; PAPANIKOLAOU and SASSI, 1989)

lenides and its Pelagonian zone is of major importance. The Pelagonian zone has been considered a fragment of the Cimmerian Continent which separated the Paleotethys from the Neotethys oceans (MOUNTRAKIS, 1986). In contrast, the present study shows that the Pelagonia terrane is part of Variscan Europe. In Greece, this zone is represented by rocks of continental affinity, located between the External Hellenides to the south and the Rhodopian units to the north (Fig. 1). The basal sequences of the Pelagonia terrane include meta-plutonic rocks considered as pre-Alpine basement (PAPANIKOLAOU and ZAMBE-TAKIS-LEKKAS, 1980; MOUNTRAKIS, 1986; SIDERIS, 1989). In order to define the age of these rocks and their significance for the evolution of Pelagonia (STAMPFLI, 1996; STAMPFLI et al., 1998), two key areas in northern and central Evia have been investigated (Fig. 2).

Previous geochronological and geochemical studies

Isotopic ages reveal the presence of pre-Alpine, especially Late Carboniferous plutonic rocks in northern and southern Greece. Most of the data concern the Internal Hellenides domain and the Attica-Cyclades Crystalline Belt (Fig. 1, Tab. 2). In the Internal Hellenides and particularly in the Flambouron unit (part of the Pelagonian basement overthrusting the neritic platform of Olympos mountain), U-Pb zircon data for the Kastania granite indicate magmatic activity around 302 Ma (YARWOOD and AFTALION, 1976). In Othrys, K-Ar hornblende ages done on amphibolites from the Pelagonian basement (FERRIÈRE, 1982), range between 332 and 307 Ma. The younger ages may represent Late Carboniferous magmatic activity, the older ages may be the result of extraneous Ar or may indicate an earlier stage of metamorphism. Meta-plutonic rocks of similar age have also been reported from the Cyclades islands (Tab. 2). These data suggest a correlation between the basement sequences of the Cyclades with those of the Internal Hellenides, rather than with the Menderes Massif which is of Panafrican origin and where Variscan metamorphic events were not recognised (SENGÖR, 1984; HETZEL et al., 1998; DANNAT and REISCHMANN, 1999) (Tab. 2). On Ios island, Rb/Sr whole rock analysis gave an age of approximately 520 Ma for granodioritic to tonalitic rocks (HENJES-KUNST and KREUZER, 1982) which is difficult to interpret due the method used and the large uncertainties ($\pm$ 55 Ma) (see ENGEL and REISCHMANN, 1998). K-Ar biotite and hornblende ages reported by HENJES-KUNST and KREUZER

(1982) range between 790 and 1600 Ma, and are possibly related to extraneous argon. These authors also report Late Carboniferous zircon ages (300–305 Ma) attributed to Variscan metamorphism, as well as Rb-Sr muscovite ages of 294 $\pm$ 4 and 288 $\pm$ 8 Ma. ANDRIESEN et al. (1987) also obtained a hornblende K-Ar age of 268 $\pm$ 27 Ma for augengneiss from the Ios gneiss dome.

Among the scarce geochemichal studies carried out on the Pelagonian basement, are those describing gneissic rocks of plutonic origin from northern Thessaly and Cyclades areas (PE-PIPER, et al., 1993; PE-PIPER and KOTOPOULI, 1997). They analyzed late Carboniferous granodiorites from Verdikoussa area in northern Thessaly and defined their chemical affinities of subduction related magma. They describe also diorites and hornblende gabbros with chemical signatures similar to continental flood basalts. These rocks were likely crystallized during Late Carboniferous but their relationships with the granodiorites are not very clear: they sometimes seem to cut them and sometimes to predate them. Amphibolites are reported from the Miocene metamorphic core complex of Naxos island as enclaves within the Variscan I-type granitoids. The metabasites resemble those found in Thessaly, with high-Ti continental flood basalts affinities, whereas the granodiorites show a subduction-related origin.

Geological setting

As shown in the structural map (Fig. 2), Evia island consists of a nappe pile comprising the following tectonic units, from south to north: (1) The formations of Ochi Mt. (Makrotantalon-Ochi unit), (2) the Styra Blueschists unit, (3) the Almyropotamos unit, (4) the Liri unit, (5) the Stropones limestones, tentatively attributed here to the external Pelagonian domain, (6) the formations of the Pelagonian zone and (7) the Vardar-Axios ophiolites (RENZ, 1955; PARROT and GUERNET, 1972; GUERNET, 1975; BAUMGARTNER and BERNOULLI, 1976; CELET and FERRIÈRE, 1978; KATSIKATSOS et al., 1986; ROBERTSON, 1990; RICHTER et al., 1996).

Field observations and samples characteristics

NORTH EVIA GRANITOIDS AND AMPHIBOLITES

The granitoids of the "basement sequences" from northern Evia form either extensive outcrops where they are found together with mica schists

and amphibolites such as in the adjacent localities of Neos Pyrgos and Aghios villages, or large stocks of unfoliated granitoids showing typical equigranular granitic texture found near Rovies (23°15' E / 38°50' N, Istiea topographic sheet, 1 : 50'000; HAGS ed. 1971) and Edipsos adjacent regions (Fig. 3). As shown by previous works the Pelagonian basement outcrops form nappes over-thusting younger metamorphic or sedimentary lithologies (SCHERMER et al., 1990). Our own

study in Edipsos and neighbouring areas con-firmed this assumption (DE BONO et al., 1999; VAVASSIS, 2000 in prep.). There is no clear intru-sive contact between the granitic bodies and the micas schists, on the contrary, all contacts appear to be syn-formational. Enclaves of mafic as well as of schistose country rocks are observed and veins and sheets of pegmatite and aplite within the country rocks are frequent, especially in Neos Pyrgos-Aghios regions. The samples are medium
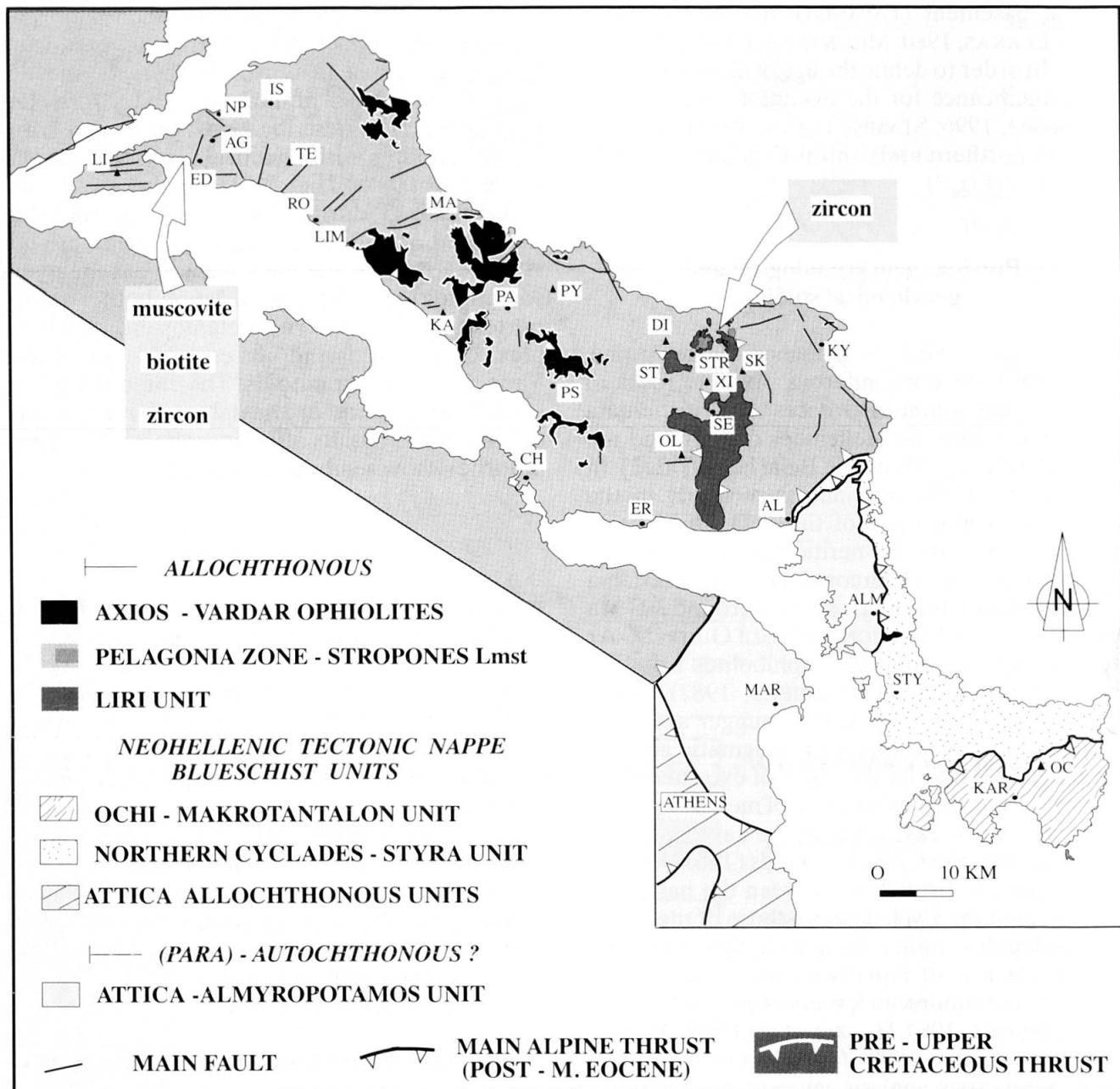
Fig. 2   Structural map of Evia island presenting the main tectonic units and the localities of the dated samples (Mod-ified from VERGELY, 1984; KATSIKATSOS, 1977a; KATSIKATSOS, 1977b; KATSIKATSOS et al., 1980; KATSIKATSOS, 1992) . AG: Aghios; AL: Aliveri; ALM: Almyropotamos; CH: Chalkis; DI: Dirfys; ED: Edipsos; ER: Eretria; IS: Istiea; KA: Kandyli; KAR: Karystos; KY: Kymi; LI: Lichas; LIM: Limni; MA: Mantoudi; MAR: Marathon; NP: Neos Pyrgos; OC: Ochi; OL: Olympos; PA: Pagondas; PS: Psachna; PY: Pyxaria; RO: Rovies; SE: Seta; SK: Skotini; ST: Steni; STR: Stro-pones; STY: Styra; TE: Telethrion; XI: Xirovouni.
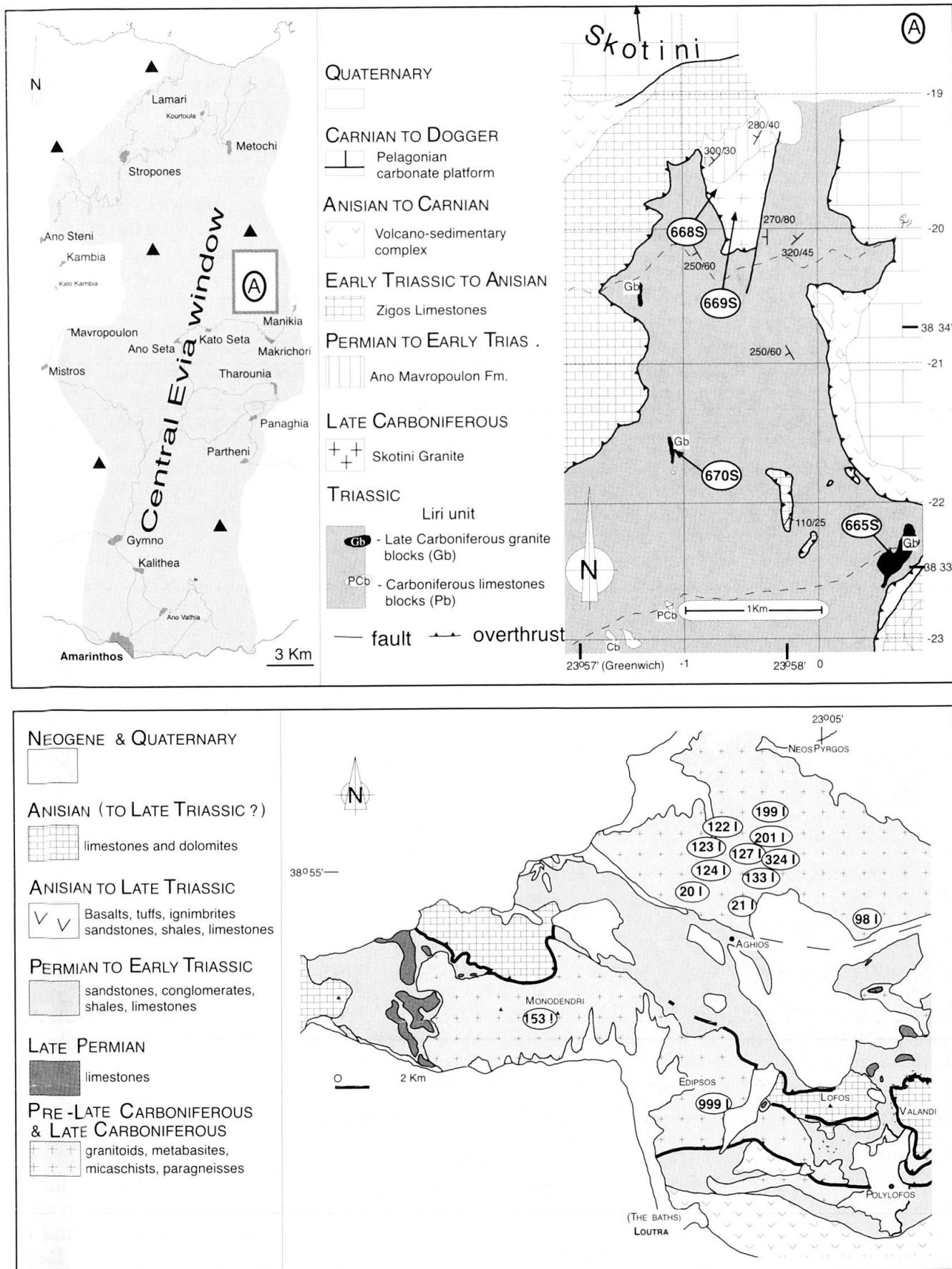
Fig. 3   Geological maps of north and central Evia regions and location of the the analyzed samples.

grained lithologies with a mineral assemblage made of saussuritized plagioclase, K-feldspar, quartz, biotite transformed to chlorite and epidote (allanite), ± muscovite, ± hornblende as well as sericite. Apatite, zircon and sphene also occur.

The analyzed meta-basic rocks represent layers or boudins obviously associated with the granites, granodiorites and gneisses of basement-type lithologies found in northern Evia. After hard efforts to find unaltered outcrops, four samples were selected from the Neos Pyrgos-Aghios region. These samples of mafic lithologies are amphibolites in close relation with the granitoids and the mica schists, and have been apparently formed within the same geotectonical context. They are found as centimeter thick-bedded horizons or boudins parallel to the dominant folliation of the host basement rocks. Mafic enclaves probably of the same origin found also within the Variscan granites have not been analyzed during this study. The Late Paleozoic age of these rocks has been confirmed by our own geochronological data (VAVASSIS, 2000 in prep.) as well as by FERRIÈRE, (1982) who reported Late Paleozoic ages for the amphibolites of the Pelagonian basement in Othrys region.

SKOTINI GRANITES

The Skotini granites (Fig. 3) were collected from the outcrops stratigraphically resting at the base of the Neopaleozoic units of central Evia (DE BONO, 1998; DE BONO et al., 1999), located about 6 km NE of Kato Seta village (Steni Dhirfios topographic sheet, 1 : 50'000; HAGS ed. 1971). They are homogeneous, coarse grained hypersolvus granites. Their typical paragenesis include quartz, albite, alkali feldspar, biotite, white mica, chlorite, stilpnomelane, titanite, apatite, zircon and calcite. Their original granitic textures are badly preserved and these rocks are usually not foliated. The Skotini granites have undergone a complex history. The study of quartz aggregates shows that there has been at least one event of static recrystallization followed by a dynamic recrystallization. Deuteric processes, such as hydrothermalism, affect the mineralogy of the rocks and resulted in the transformation of feldspaths to sericite and kaolinite and the formation of veins of stilpnomelane, quartz, aciculate white micas, chlorite and calcite. Biotite is usually altered to chlorite and associated with neoformed stilpnomelane. Almost every mineral show undulate extinction and deformation features such as lamellae in quartz. Hence these granites went through low-grade metamorphic conditions.

LIRI GRANITES

The samples from Liri (Fig. 3) come from olistoliths belonging to the Permo-Triassic Liri unit, situated about 3.5 km in the NE of Kato Seta village or 1 km west of Manikia village (Steni Dhirfios topographic sheet, 1 : 50'000; HAGS ed. 1971). The granitic blocks and pebbles included in the Liri flyschoid sequence are mineralogically similar to the granites from Skotini. However, small differences exist: Liri granites are less affected by deuteric processes and some samples have not been affected by static recrystallization.

Geochemistry

Together with the zircon typology described thereafter, 26 granitic rocks and amphibolites have been analysed for major and trace element chemistry in order to characterise the geotectonic setting of the Pelagonia Terrane (Tab. 1).

MAJOR ELEMENTS

Because all samples underwent several deformation events, low to medium grade metamorphism, including weathering and late hydrothermal alteration for some of them, we expected element mobility to induce changes in the rock bulk chemistry. This was confirmed by field and petrographic observation as well as by the results of the major elements analyses, which show, for almost all the samples, unusually high content in K_2O and low content in Na_2O.

TRACE ELEMENTS

Interpretations based on trace elements and rare earth elements are considered useful. The granitoid samples, when plotted on a Rb vs. Y+Nb discriminative diagram (Fig. 4a), show a "volcanic arc granite" affinity, also shown by the Nb -Y diagram. Multitrace element variations, normalized to ocean ridge granites (ORG), indicate also calc-alkaline affinities for the Liri, Skotini and Edipsos granitoids (Fig. 4b).

The negative anomalies in Nb may be due to continental crust contamination. Most of the samples show similar normalized values of Ba and Th typical of Within Plate Granites (WPG). Relatively low normalized contents in K_2O and Ba together with peaks of Rb and Th and a negative anomaly in Hf, indicate collisional granites. Additionally, the observed positive anomaly in Ce and
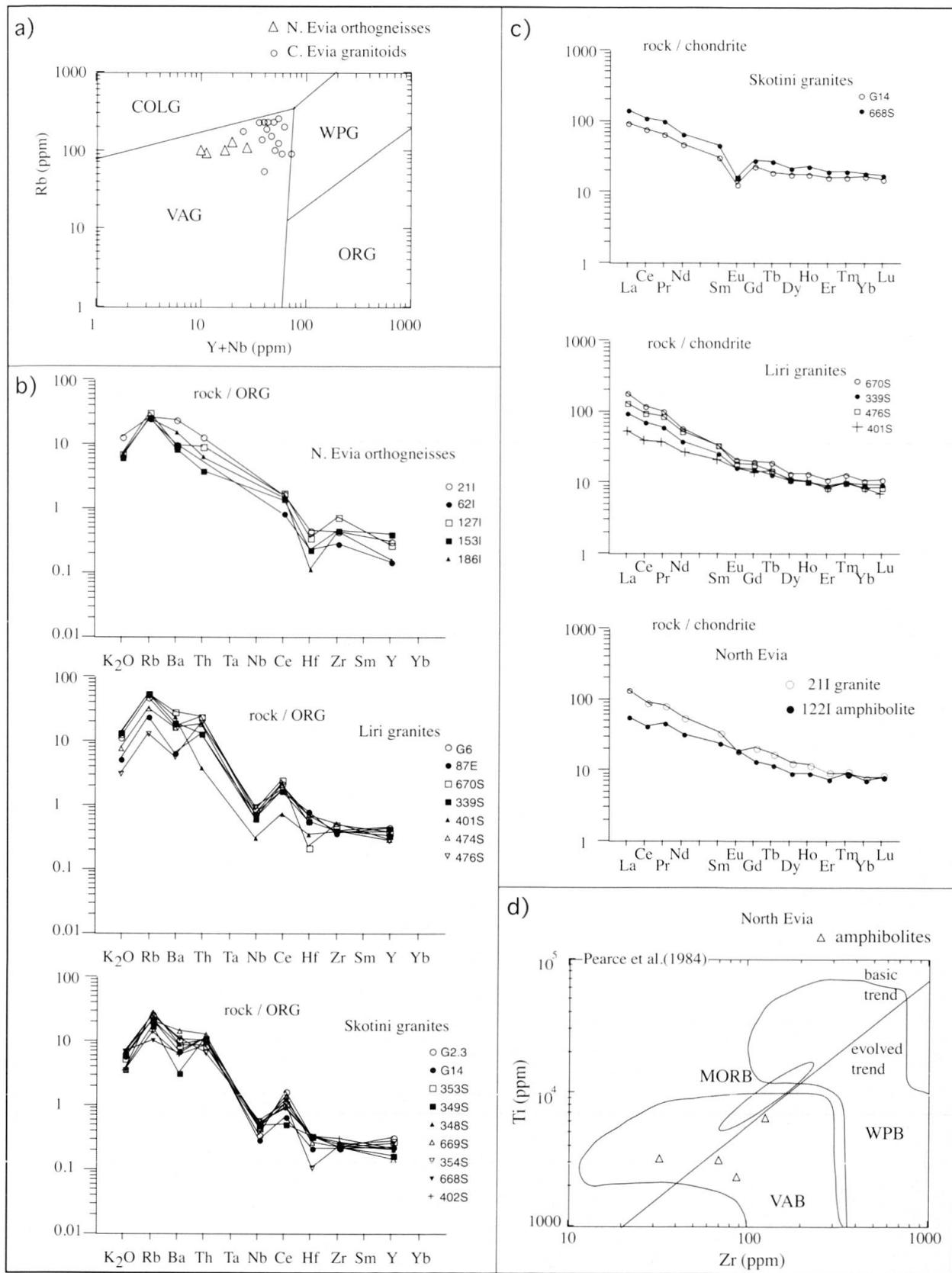
Fig. 4

Fig. 4 Geochemical discrimination and spider diagrams of the analyzed rocks. (a) Rb vs Y + Nb discriminative diagram after PEARCE et al. (1984); VAG: volcanic-arc granites; COLG: collisional granites; WPG: within-plate granites; ORG: ocean ridge granites. (b) Ocean-ridge granite (ORG)-normalized spider-diagrams after PEARCE et al (1984). (c) REE patterns; normalization values from HASKIN et al. (1968) and NAKAMURA (1974). (d) Ti vs Zr discriminative diagram after PEARCE (1982); VAB: volcanic-arc basalts; MORB: middle ocean ridge basalts; WPB: within-plate basalts.

Tab. 1 Whole rock geochemical analyses of Evia samples.

| | N. Evia amphibolites & orthogneisses | | | | | | | | | C. Evia Skotini granites | | | | | | | | |
| | amphibolites | | | | orthogneisses | | | | | | | | | | | | | |
samples	20I	122I	123I	124I	21I	62I	127I	153I	186I	G2.3	G14	668S	349S	348S	669S	354S	505S	402S
major wt-%																		
SiO2	50.25	53.59	49.33	49.55	77.85	69.23	65.39	63.38	65.62	68.34	68.69	68.48	65.82	67.6	68.12	68.46	63.93	68.17
TiO2	0.52	0.53	1	1.16	0.11	0.38	0.74	0.58	0.48	0.44	0.40	0.42	0.53	0.44	0.41	0.4	0.49	0.5
Al2O3	16.46	12.79	16.23	20.55	12.33	15.68	16.7	16.59	16.44	15.83	16.06	15.6	16.89	15.71	15.9	15.49	17.49	15.24
Fe2O3	8.48	8.46	10.61	10.14	0.87	3.1	4.18	4.66	3.87	2.94	2.96	3.6	4.15	3.78	3.32	3.43	4.23	4.58
FeO										0.81	0.37							
MnO	0.13	0.14	0.15	0.12	0	0.04	0.03	0.06	0.06	0.06	0.02	0.06	0.03	0.05	0.05	0.04	0.07	0.05
MgO	7.65	9.71	5.36	4.1	0.34	1.02	0.98	1.91	1.35	1.27	1.22	1.62	2.24	1.23	1.29	1.28	1.67	1.66
CaO	10.34	8.16	9.5	7.77	0.61	2.5	2.54	3.33	2.49	0.19	0.23	0.14	0.04	0.17	0.16	0.13	0.07	0.31
Na2O	2.34	1.09	1.35	1.25	2.21	3.79	3.47	3.88	4.17	2.35	3.24	2.48	4.38	5.46	2.59	1.79	2.37	3.24
K2O	1.56	2.94	2.63	4.03	4.87	2.49	2.65	2.42	2.62	5.23	4.77	4.34	3.01	3.00	5.71	5.78	5.56	2.88
P2O5	0.04	0.13	0.15	0.26	0.02	0.07	0.23	0.11	0.14	0.13	0.12	0.1	0.13	0.16	0.08	0.18		
LOI	2.07	2.04	2.88	0.22	0.77	1.6	2.14	2.6	1.95	2.13	1.70	2.39	2.79	1.71	2.12	2.16	3.08	2.27
Cr2O3	0.03	0.12	0.01	0.00	0.00	0.00	0.00	0.00	0.00	0.00	0.00	0.00	0.00	0.00	0.00	0.00	0.00	0.00
NiO	0.01	0.03	0.00	0.00	0.00	0.00	0.00	0.00	0.00	0.00	0.00	0.00	0.00	0.00	0.00	0.00	0.00	0.00
Total	99.88	99.73	99.2	99.15	99.98	99.9	99.05	99.52	99.19	99.72	99.77	99.26	99.98	99.28	99.83	99.07	99.04	99.09
traces (ppm)																		
Nb	0	0	0	2	0	0	0	0	0	7	6	9	10	11	9	12	10	11
Zr	32	75	87	131	140	94	236	149	141	157	146	171	157	188	154	159	156	210
Y	14	12	23	30	21	10	18	27	11	45	32	40	24	30	21	29	36	31
Sr	109	115	488	521	159	254	388	197	203	40	56	30	38	47	65	53	76	84
U	0	0	0	3	0	0	0	0	0	3	2	4	6	4	4	3	4	4
Rb	88	135	126	151	101	96	121	101	96	207	178	178	139	233	166	207	82	113
Th	0	4	2	9	10	0	7	3	5	17	18	14	18	17	21	11	18	14
Pb	0	0	0	0	30	0	0	0	0	35	28	27	31	30	37	22	24	17
Ga	12	11	11	19	15	17	19	17	15	20	18	19	20	21	19	18	18	18
Zn	75	86	89	121	20	43	68	62	51	59	59	51	63	72	50	53	66	57
Cu	0	0	0	0	0	0	0	0	0	13	10	14	11	11	9	7	16	12
Ni	77	166	4	0	0	0	1	1	0	6	4	5	5	9	4	5	4	7
Co	52	46	46	51	26	35	32	29	28	28	28	35	29	38	45	32	31	46
Cr	216	862	73	16	0	7	6	15	13	25	18	16	22	18	17	18	23	17
V	194	190	281	297	3	56	67	97	65	56	46	53	94	62	49	51	62	81
Ce	0	31	29	65	56	28	59	48	54	116	47	75	36	67	98	76	87	63
Nd	0	13	8	33	15	1	22	21	17	79	26	36	15	36	45	40	33	27
Ba	99	505	325	987	1130	475	452	411	744	1110	721	882	320	921	1473	1149	635	613
La	0	18	10	43	33	13	38	25	33	84	33	39	24	46	64	43	39	32
S	68	81	66	72	55	34	39	38	34	7	8	14	3	67	68	28	2	26
Hf	0	0	0	1	4	2	3	2	1	6	4	6	6	6	5	2	6	6
Sc								<0<	<0<	7	7	5	7	6	6	6	10	13
As								<0<	<0<	<3<	<3<	3	<0<	4	3	6	11	27

| | C. Evia Liri granites | | | | | | |
samples	G6	87E	670S	339S	401S	474S	476S
major wt-%							
SiO2	68.86	72.61	62.96	63.26	64.3	61.98	68.19
TiO2	0.40	0.21	0.66	0.6	0.72	0.65	0.33
Al2O3	14.90	14.89	16.06	16.49	18.09	16.76	13.35
Fe2O3	2.94	2.41	5.04	4.92	4.37	5.26	2.3
FeO	0.38						
MnO	0.06	0.03	0.08	0.08	0.04	0.08	0.05
MgO	1.31	0.92	2.79	2.93	1.87	2.51	1.06
CaO	0.31	0.19	2.49	2.24	0.33	2.34	3.95
Na2O	3.61	4.39	1.39	1.59	1.68	2.76	4.88
K2O	4.38	1.99	5.07	5.09	5.04	3.01	1.18
P2O5	0.13	0.07	0.16	0.14	0.26	0.11	0.13
LOI	2.11	1.68	2.67	2.75	2.83	4.05	4.09
Cr2O3	0.00	0.00	0.01	0.00	0.01	0.01	0.00
NiO	0.00	0.00	0.00	0.00	0.00	0.00	0.00
Total	99.39	99.39	99.38	100.1	99.54	99.52	99.51
traces (ppm)							
Nb	7	7	8	6	3	6	9
Zr	130	122	165	129	123	169	132
Y	31	30	26	23	26	20	19
Sr	98	53	128	240	43	135	303
U	2	3	3	3	2	3	1
Rb	183	91	209	205	210	125	49
Th	18	10	18	10	3	14	15
Pb	34	15	13	16	7	12	14
Ga	18	15	20	21	23	20	13
Zn	51	41	67	62	55	69	36
Cu	8	11	10	11	10	18	8
Ni	4	4	14	13	19	16	1
Co	30	81	46	49	46	41	47
Cr	18	10	46	40	49	61	12
V	51	37	103	100	117	143	43
Ce	72	57	83	56	25	70	59
Nd	33	23	40	27	13	38	28
Ba	799	309	1329	905	1146	776	276
La	42	21	70	38	24	31	31
S	<3<	<0<	7	8	14	<0<	5
Hf	5	7	2	5	3	6	6
Sc	9	6	9	8	5	13	8
As	4	5	7	4	23	12	4

| | N.Evia granites & amphibolites | | C.Evia Skotini granites | | C.Evia Liri granites | | | |
| samples | 21I | 122I | G14 | 668S | 339S | 670S | 476S | 401S |
REE (ppm)	granite	amphib.						
La	48.8	20.2	30.7	46.9	30.1	58.6	42.2	17.8
Ce	84.3	38.9	65.6	92.9	59.9	101	81.3	33.6
Pr	10.4	5.8	7.4	11.5	6.8	11.5	9.7	4.3
Nd	37.7	22	29.6	40.5	23.2	36.3	32.2	16.7
Sm	7.6	5.2	6.2	9.2	5.1	6.6	6.6	4.2
Eu	1.55	1.57	0.99	1.22	1.21	1.61	1.38	1.24
Gd	6.2	4	6.4	7.6	4.1	5.4	4.9	3.9
Tb	0.9	0.6	0.9	1.3	0.6	0.9	0.7	0.7
Dy	4.8	3.4	6	7.4	3.6	4.5	3.7	3.8
Ho	0.94	0.69	1.25	1.62	0.71	0.93	0.71	0.75
Er	2.2	1.8	3.6	4.3	2	2.4	1.9	1.9
Tm	0.3	0.3	0.5	0.6	0.3	0.4	0.3	0.3
Yb	1.9	1.7	3.6	4	2	2.3	1.8	1.8
Lu	0.29	0.29	0.51	0.58	0.31	0.37	0.28	0.23
Th	18.3	8.2	16.8	18.9	13.3	28.7	17.7	1.7
U	2.9	2.4	3.2	3.5	2.6	2.8	1.8	1.1

Tab. 2 Zircon geochronological data of Paleozoic-Early Mesozoic magmatism in Greece and W. Turkey.

No	Place or Unit	Age in Ma	Method	References
1	Pangeon-Sidironero (Rhodope)	345 ± 40	Pb/Pb	KOKKINAKIS (1978)
2	Thassos (Rhodope)	300	U-Pb	WAWRZENITZ (1997)
3	Flambouron	302 ± 5	U-Pb	YARWOOD and AFTALION (1976)
4	Evia	308 - 319	U-Pb	This study
5	Dilos	295 ± 4 - 327 ± 4	Pb/Pb	ENGEL and REISCHMANN (1999)
6	Paros	302 ± 2 - 325 ± 4	Pb/Pb	ENGEL and REISCHMANN (1999)
7	Antiparos	292 ± 1 - 308 ± 3	Pb/Pb	ENGEL and REISCHMANN (1999)
8	Naxos	316 ± 4 275 ± 3 233 ± 2	Pb/Pb	REISCHMANN (1998)
9	Sikinos	301 ± 2 - 325 ± 4	Pb/Pb	REISCHMANN (1998)
10	Ios	305 ± 5 302 - 311	U-Pb Pb/Pb	HENJES-KUNST and KREUZER (1982) ENGEL and REISCHMANN (1999)
11	Kazdag (Sakarya)	308 ± 16 399 ± 13	Pb/Pb	OKAY et al. (1996)
12	Bozdag (Menderes)	551 ± 1.4	U-Pb	HETZEL et al. (1998)
13	Menderes	528 - 541 227 - 240	Pb/Pb	DANNAT and REISCHMANN (1998)

the slightly negative anomaly in Ba in most of the samples point to a volcanic arc setting (VAG).

REE patterns show high LREE enrichment and a moderately fractionated pattern (Fig. 4c). The negative Eu anomaly is distinct and indicates segregation of feldspar, except for the Liri granitoids where this anomaly is small.

The amphibolitic samples, except sample 124I, show low content in Nb (< 1 ppm) often characteristic for subduction zone basalts (Tab. 1). For sample 122I the Rare Earth elements spectrum normalized to chondrites, clearly shows an enrichment in light elements, probably due to crustal contamination (Fig. 4c). The flat pattern with chondrite-normalized factors of about 10 for HREE is similar to patterns of either MORB-type basalts or subduction zone basalts. On the Ti-Zr discriminative diagram for volcanic rocks, all amphibolitic samples plot in the field of Volcanic Arc Basalts (VAB) (Fig. 4d).

Zircon typology

The basis of this empirical method is to determine what kind of prisms {100} or/and {110} and what pyramids {211} or/and {101} the zircon has developed. The growth of these crystal faces is roughly controlled by the agpaicity index (index I.A.). (PUPIN, 1976), the temperature of crystallization and the percentage of water in the magma (index I.T.) (PUPIN, 1978; PUPIN and TURCO, 1972). It is

Tab. 3 U-Pb data for Evia samples. (a) total common Pb in fraction; (b) model Th/U ratio calculated from radiogenic $^{208}Pb/^{206}Pb$ ratio and $^{208}Pb/^{238}U$ age; (c) the $^{208}Pb/^{204}Pb$ and $^{207}Pb/^{204}Pb$ ratios are corrected for spike and fractionation, but not for procedure blank; (d) atomic ratios corrected for blank, spike, fractionation and initial common Pb when present; error estimates (95 % confidence level) refer to the last significant digits of the isotopic ratios and reflect reproducibility of standards, measurement errors and uncertainties in the common Pb correction.

# number of grains	Mass (mg)	U ppm a	ComPb pg	Th/U (model) b	206Pb/204Pb c	206Pb/238U d	207Pb/235U d	207Pb/206Pb d	206Pb/238U	207Pb/235U	207Pb/206Pb
Rovies metagranodiorite - 186 I											
1 (1)	23	358	1.23	0.16	21147	0.05001 ± 24	0.3640 ± 19	0.05279 ± 12	314.6	315.2	319.8
2 (2)	33	228	1.37	0.15	17324	0.05001 ± 10	0.3638 ± 8	0.05276 ± 5	314.6	315.1	318.4
3 (3)	32	267	5.43	0.26	4966	0.05000 ± 14	0.3638 ± 11	0.05277 ± 7	314.5	315.1	318.9
4 (3)	26	370	2.38	0.19	12941	0.05083 ± 11	0.3703 ± 9	0.0528 ± 6	319.6	319.9	321.8
Edipsos metagranite - 153 I											
5 (4)	40	287	1.83	0.38	19415	0.04906 ± 15	0.3556 ± 16	0.05258 ± 17	308.7	309.0	310.5
6 (4)	32	338	2.67	0.46	12495	0.04889 ± 32	0.3556 ± 26	0.05275 ± 17	307.7	308.9	318.3
7 (3)	28	522	3.24	0.34	13926	0.04904 ± 12	0.3553 ± 10	0.05254 ± 6	308.6	308.7	308.9
8 (2)	20	489	2.77	0.31	10876	0.04892 ± 9	0.3545 ± 8	0.05256 ± 6	307.9	308.1	309.8
Skotini granite - 668S											
9 (1)	16	165	0.73	0.26	11558	0.05089 ± 11	0.3720 ± 10	0.05302 ± 8	320.0	321.1	329.7
10 (1)	11	110	0.62	0.36	6966	0.05656 ± 12	0.4250 ± 14	0.05450 ± 13	354.7	359.6	391.7
11 (1)	5	328	0.98	0.31	33678	0.07506 ± 20	0.6474 ± 22	0.06255 ± 12	466.6	506.9	693.1
12 (1)	3	163	0.58	0.41	7944	0.05026 ± 20	0.3658 ± 32	0.05279 ± 39	316.1	316.6	319.8
13 (1)	4	135	0.97	0.43	8256	0.05231 ± 36	0.3861 ± 59	0.05353 ± 50	328.7	331.5	351.3
Skotini granite - 669S											
14 (1)	12	44	0.78	0.44	2157	0.05026 ± 35	0.3657 ± 45	0.05277 ± 50	316.1	316.5	319.0
15 (3)	23	237	1.26	0.23	13959	0.05125 ± 11	0.3835 ± 10	0.05427 ± 7	322.2	329.6	382.5
16 (3)	12	339	2.66	0.32	4840	0.05011 ± 14	0.3634 ± 15	0.05260 ± 14	315.2	314.8	311.6
17 (3)	13	284	1.94	0.33	6415	0.05330 ± 14	0.3959 ± 15	0.05388 ± 13	334.7	338.7	365.9
Liri granite - 670S											
18 (2)	10	310	2.14	0.42	4599	0.05016 ± 15	0.3647 ± 16	0.05274 ± 17	315.5	315.7	317.5
19 (4)	20	367	3.30	0.45	7013	0.04987 ± 11	0.3625 ± 10	0.05272 ± 8	313.7	314.1	316.8
20 (4)	17	196	0.73	0.44	14313	0.04976 ± 9	0.3616 ± 10	0.05269 ± 6	313.1	313.4	315.6
21 (2)	13	389	2.80	0.44	5619	0.04926 ± 13	0.3574 ± 12	0.05262 ± 11	310.0	310.3	312.6
22 (4)	12	342	4.80	0.58	2683	0.04960 ± 13	0.3598 ± 13	0.05262 ± 13	312.0	312.1	312.5
Liri granite - 665S											
23 (1)	8	432	3.23	0.44	3362	0.04960 ± 15	0.3603 ± 16	0.05269 ± 16	312.1	312.5	315.4
24 (5)	21	189	1.32	0.30	10175	0.05364 ± 14	0.4051 ± 13	0.05477 ± 9	336.9	345.4	402.9
25 (2)	9	356	1.29	0.40	7572	0.04833 ± 12	0.3503 ± 11	0.05257 ± 9	304.3	305.0	310.2
26 (1)	4	502	5.50	0.43	1575	0.04930 ± 21	0.3580 ± 25	0.05267 ± 27	310.2	310.7	314.6
27 (1)	3	787	3.40	0.41	3916	0.04903 ± 18	0.3557 ± 22	0.05261 ± 24	308.6	309.0	312.1
28 (1)	3	744	1.30	0.41	12535	0.04928 ± 12	0.3575 ± 13	0.05261 ± 13	310.1	310.7	311.9

also controlled by the rate of crystallization and by chemical substitutions in the lattice (BENISCHEK and FINGER, 1993; VAVRA, 1992). The partition of the population in the typologic diagram and typological evolution trend (T.E.T.) for the sample, give information about their magmatic evolution (Fig. 5). Nine samples, with a population of 100 unbroken zircons per sample, were studied by scanning microscopy (SEI mode). Data are shown in the discriminant diagram of PUPIN, (1988) (Fig. 6). Seven samples are from central Evia (668S, 669S 665S, 670S, G2, G6, G14), and two samples from the northern part of the island (153I from Edipsos and 186I from the Rovies region).

The typologic study of zircon population was undertaken to better define the petrogenesis of granitic rocks from Evia and to assess the polygenic nature of the granitic basement. As zircon is stable in near-surface environments this method is quite useful for granitic rocks which experienced hydrothermal alteration and weathering affecting their chemical and mineralogical composition. All samples from central Evia converge towards the G characteristic of late crystallization stages (PUPIN, 1980). Sample 668S is an especially well differentiated granite with over 40% of G type zircons. Samples G2, G6, G14, 665S, 669S and 670S contain smaller amounts of G type zircons.

In northern Evia both samples 153I and 186I show poorly evolved (or early) zircons with predominant {100} prisms; sample 186I being more differentiated. It is not clear in which environment these rocks crystallized. However, the {211} pyramids are well developed in both samples. In the discriminant diagram (Fig. 6) all samples plot in the field of calc-alkaline granites, except G2 which is found in the domain of the aluminous monzogranites.

Distribution percentage
of zircon types
☐ 0-2 %
▨ >2-5 %
▨ >5-10 %
▨ >10-20 %
■ >20-40 %
■ >40 %
- - - - - - -
Mean point :
● : (I.A / I.T)

Sample : G2   I.A.   I.T. 390; IA: 365
Sample: 670S   I.A.   IT: 460; IA: 455
Sample: 665S   I.A.   IT: 400; IA: 600
Sample: G6   I.A.   IT: 365; IA: 440
Sample: 669S   I.A.   IT: 360; IA: 555
Sample : 153I   I.A.   IT: 630; IA: 440
Sample : G14   I.A.   IT: 370; IA: 470
Sample: 668S   I.A.   IT: 340; IA: 600
Sample : 186I   I.A.   IT: 570; IA:3 90
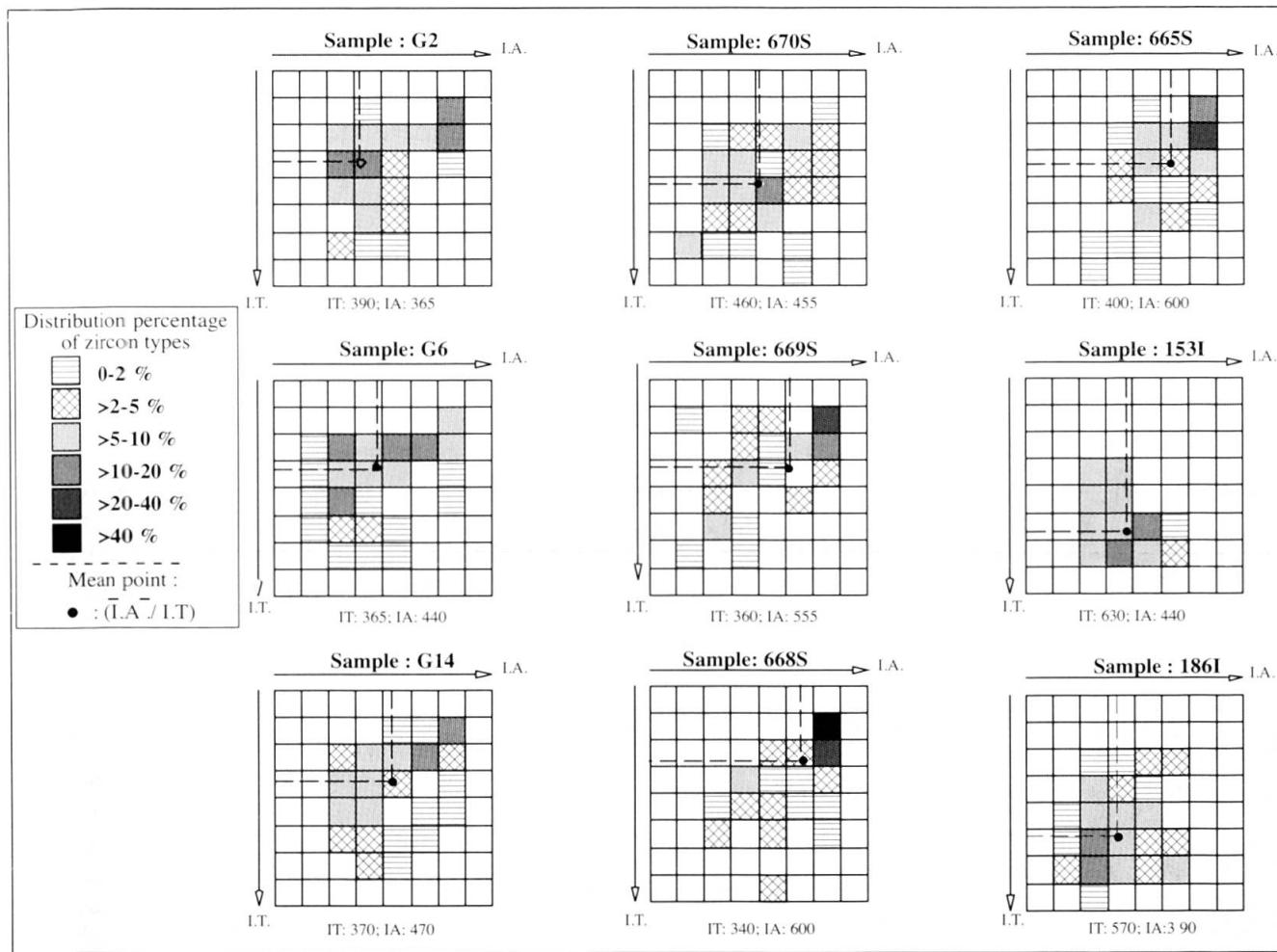
Fig. 5   Typologic distribution diagrams and A/T coordinates (PUPIN, 1980) for the analyzed samples. Each sample corresponds to 100 zircons analyses.

Results of U-Pb dating

Zircon used for U/Pb data have been isolated using conventional heavy liquid and magnetic separation techniques. Chemistry and measurements were made following the conventional procedure developed at the Royal Ontario Museum (KROGH, 1973).

Air-abrasion was applied systematically to reduce or eliminate surface-correlated lead loss and younger overgrowths (KROGH, 1982). U-Pb analytical data for zircon fractions are presented in table 3 and in figure 7.

ROVIES GRANITE

Sample 186I
Zircons are euhedral and pale-brown in colour. There is no evidence for inherited components. Most of the obtained zircon ages are slightly discordant (fractions [1], [2], [3]) with a $^{206}Pb/^{238}U$ weighted mean value at 314.6 ± 0.5 Ma and a $^{207}Pb/^{206}Pb$ mean age of 318 ± 0.5 Ma. The fourth fraction is concordant at 319.6 ± 0.4 Ma (Fig. 7A). The most likely interpretation is that the concordant age of fraction [4] at 319.6 ± 0.7 Ma is the crystallization age and the remaining fractions are affected by a slight Pb loss.

EDIPSOS GRANITE

Sample 153I
Zircons from this sample are pink in colour, but are similar to the other samples in terms of habit, U concentrations and Th/U ratios. The analyzed zircon fractions [5], [7], [8] are concordant or close to Concordia providing a $^{206}Pb/^{238}U$ weighted mean value of 308.3 ± 0.4 Ma, interpreted as the crystallization age of the granite. (Fig. 7B). Fraction [6] is subconcordant at a similar U-Pb apparent age.
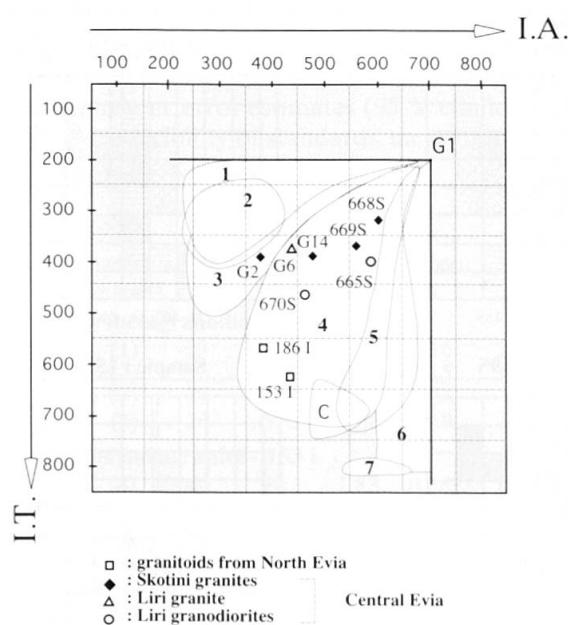
Fig. 6 Discriminant diagram for the north and central Evia granites and principal granitic types according to their zircon populations (PUPIN, 1988).
Crustal origin: (1) Autochthonous and intrusive aluminous leucogranite; (2) (Sub)-autochthonous monzogranites and granodiorites; (3) Intrusive aluminous monzogranites and granodiorites.
Hybrid origin: (4) Calk-alkaline series granites; (5) Subalkaline series granites. Continental tholeiitic granites. Granites of mantle or mainly mantle origin; (6) Alkaline series granites; (7) Tholeitic series granites.

SKOTINI GRANITES

Sample 668S

Among the five analyzed fractions [9–13], [12] is concordant within one σ error at a mean U-Pb age of 316 ± 1.3 Ma. All other fractions have higher apparent U-Pb ages pointing to lead inheritance. Three of them [9, 10 and 13] are collinear together with [12] (MSWD = 0.071), defining a discordia line with lower and upper intercept ages of 311 ± 4.1 and 612 ± 47 Ma, respectively (Fig. 7C). Relying preferentially on the concordant data point, 316 ± 1.3 Ma is interpreted as the best estimated crystallization age of the 668S Skotini granite, whereas the upper intercept age of 600 Ma point to a Pan-African component in the source material of the magma. Fraction [11] (not shown in Fig. 7C) has a much higher $^{207}Pb/^{206}Pb$ apparent age (693 ± 4 Ma) than all other fractions, pointing to an additional inherited component about 1025 Ma old (upper intercept age of a discordia line drawn through fractions [12] and [11]).

Sample 669S

This sample yielded two concordant zircon fractions, [14] and [16], with a weighted mean $^{206}Pb/^{238}U$ age of 315.3 ± 0.8 Ma (Fig. 7D and Tab. 3). This is considered to be the best estimate for the timing of crystallization; this age is identical within error to that obtained on sample 668S. Two other fractions, [15] and [17] show the presence of different inherited components of Mesoproterozoic to Neoproterozoic ages.

LIRI GRANITES

Sample 670

Five multigrain zircon analyses are concordant with $^{206}Pb/^{238}U$ ages between 310.0 ± 0.8 Ma and 315.5 ± 0.9 Ma (Fig. 7E, Tab. 3). These data provide no indication for the presence of a much older component from the basement. A possible interpretation could be a protracted crystallization with a minimum duration of ca. 5 Ma, possibly as a result of multiple magma injection. More realistically, a slight lead loss and/or inheritance effect is probably hidden within the error ellipses. Fraction [21] for instance (Fig. 7E), which has the same $^{207}Pb/^{206}Pb$ age as the perfectly concordant fraction [22], might well have slightly shifted down in response to a residual lead loss incompletely removed by the air abrasion process. Alternatively, [18] might incorporate a very small inherited component. To stay on the safe side, we consider the crystallization time of the Liri granite 670S to be in the age range of 310 to 315 Ma.

Sample 665 S

The single grain fractions [23], [26], [27] and [281 are euhedral, brown, elongated prismatic grains, containing multiple small fluid inclusions distributed uniformly through the grain volume (Fig. 7F). No features that are usually related to the presence of a core (e.g. variations in color, turbid spots, radial fractures etc.) were detected. They are all concordant between $^{206}Pb/^{238}U$ ages of 308.6 and 312.1 Ma, but do not completely overlap within errors. A slight lead loss and /or inheritance effects could be responsible for this discrepancy, but can hardly be evidenced. Consequently we propose a mean value of 310 ± 3 Ma for the crystallization age of the Liri granite block. The other analyzed fractions are discordant and point either to inheritance [24] or lead loss [25].

$^{40}Ar/^{39}Ar$ Mica geochronology

Muscovite and biotite were selected and analyzed at the University of Lausanne by conven-
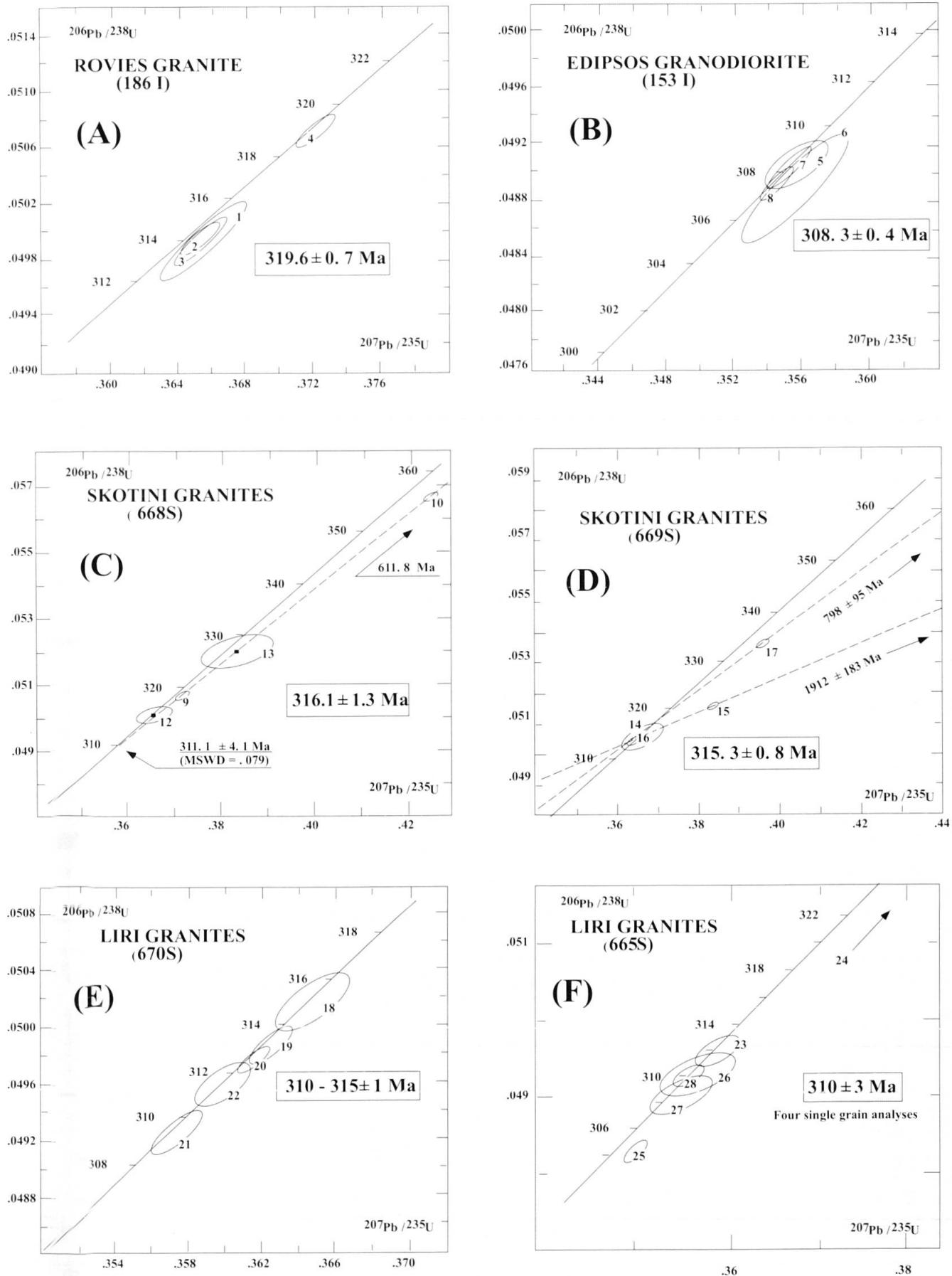
Fig. 7'   U-Pb concordia diagram for zircon from granites of northern and central Evia. Errors of the ages are quoted at the 95% confidence level; 2σ uncertainties are shown as error ellipses. In the figures, upper concordia intercept ages are indicated with black arrows. The ages that are considered reliable ages of crystallization are framed.

tional $^{40}Ar/^{39}Ar$ furnace step methods (for details about the analytical procedures, see COSCA et al., 1998).

Muscovite and biotite samples of micaschist and gneisses have been selected in order to estimate the age of the metamorphic event(s) recorded in the northern part of Evia island.

The results of the $^{40}Ar/^{39}Ar$ step heating experiments are presented in Fig. 8. Data obtained for muscovite of the less deformed samples 999I and 199I from Edipsos and Aghios indicate plateau and near plateau dates at 297.1 ± 0.3 Ma and 288 Ma respectively (Fig. 8b). In addition, an isochron plot (MSWD = 1.2) of sample 999I excludes the presence of excess argon ($^{40}Ar/^{36}Ar$ ratio = 295.5). However muscovite $^{40}Ar/^{39}Ar$ spectra of samples 324I, 201I, 98I, and 133I from Aghios – Neos Pyrgos region did not allow a strict calculation of an age plateau (Fig. 8a) and the in-

tegrated dates range from 272 to 290 Ma for all these deformed samples. The data are tightly clustered when plotted on an isochron diagram, precluding an independent check on the isotope composition of the nonradiogenic argon. The staircase shaped conventional $^{40}Ar/^{39}Ar$ spectra are consistent with some Ar loss in mylonitic gneisses and deformed micaschists, whereas the less deformed plutonic rocks yield flat age spectra. Similar patterns have been interpreted to reflect argon loss concentrated in shear bands within the mica of rocks having experienced simple shear deformation and metamorphism at low to moderate temperatures (KRAMAR et al., 1998). This simple shear deformation could be Variscan or younger.

Two biotites from the same samples used for muscovite analysis (324I and 201I) have been analyzed. The biotites yielded highly perturbed
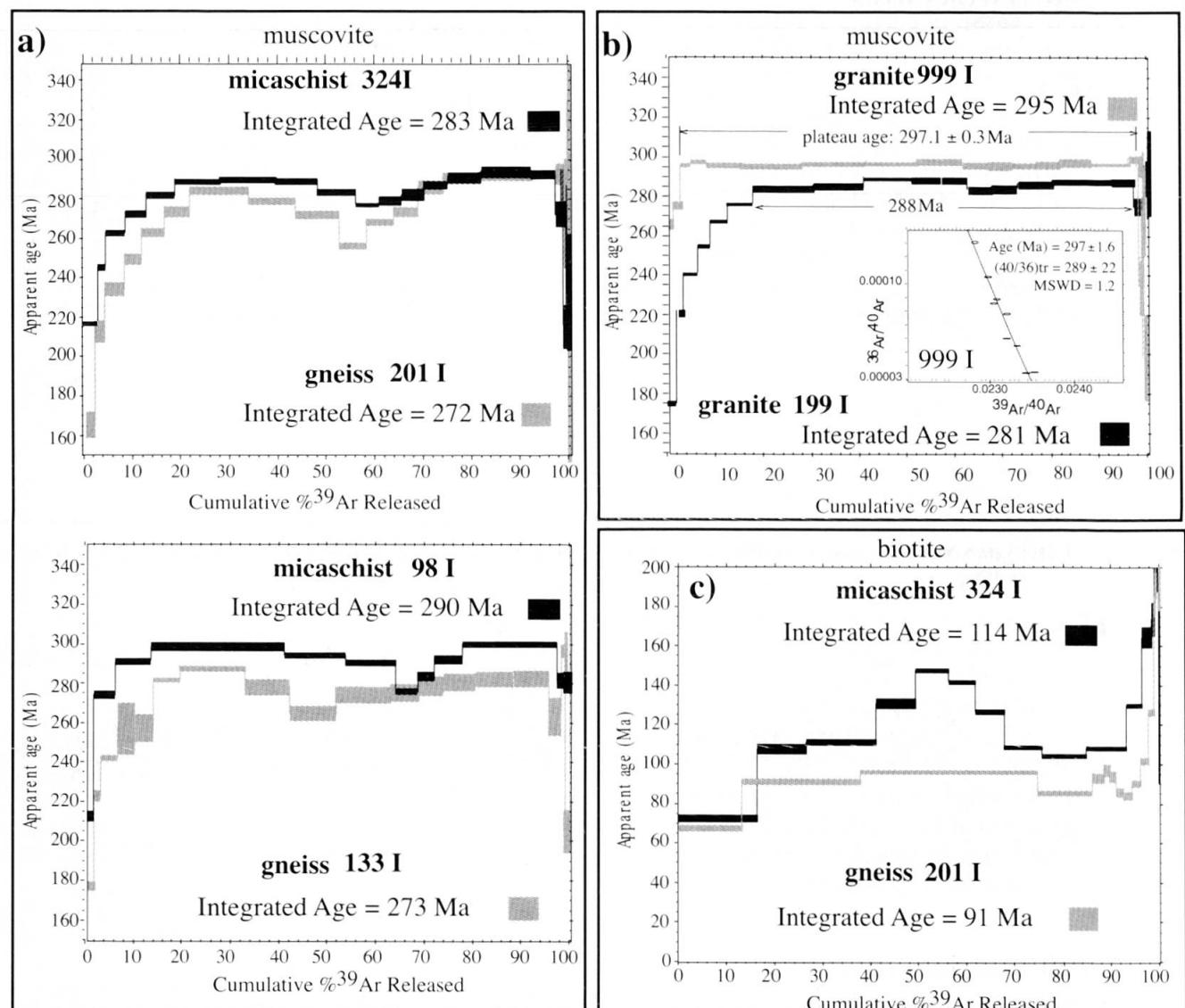
Fig. 8 $^{40}Ar/^{39}Ar$ age spectra of muscovite and biotite from micaschists and metagranitoids from Aghios, Neos Pyrgos and Edipsos (north Evia). Analytical data can be obtained from the authors upon request.

spectra (Fig. 8c), with integrated dates of 113.6 Ma and 91.1 Ma. These dates are not considered geologically meaningful and possible explanations for this kind of $^{40}Ar/^{39}Ar$ degassing shape are: (1) partial argon resetting of pre-Alpine biotites during the Alpine orogenic event, (2) excess argon in Alpine biotites, (3) partial mixture of Alpine and pre-Alpine biotites and (4) ^{39}Ar recoil effects associated with interlayered chlorite.

To summarize geochronological data, we interpret the $^{40}Ar/^{39}Ar$ muscovite data of samples 999I and 199I to record regional metamorphic cooling below temperatures of about 400 °C (KIRSCHNER et al., 1996) at 288–297 Ma.

Discussion and geodynamic implications

The basement rocks from Evia represent the Pelagonia continental crust consolidated during Carboniferous time. Figure 9 shows a compilation of the most recently dated intrusive bodies of Evia (this paper), Flambouron (YARWOOD and AFTALION, 1976), Olympos mountain (SCHERMER et al., 1990), Othrys mountain (SMITH et al., 1975; SMITH et al., 1979; FERRIÈRE, 1982), the Cyclades (HENJES-KUNST and KREUZER, 1982; REISCHMANN, 1998; ENGEL and REISCHMANN, 1998; ENGEL and REISCHMANN, 1999) and other basement sequences in the Internal Hellenides (Serbomacedonian) which have similar Early Permian to Late Carboniferous ages (BORSI et al., 1966). The Rhodope intrusives (Pangeo, Sidironero) yield identical as well as slightly older Early Carboniferous ages (KOKKINAKIS, 1978; WAWRZENITZ, 1997) whilst Triassic ages have been found on Naxos (REISCHMANN, 1998) and Crete (SEIDEL et al., 1982). This Pelagonian type basement extends northwestward to Croatia where PAMIC et al., (1996) describe I-type together with S-type granitoids of Late Carboniferous age. Together with our own data, they confirm the extension of a Variscan cordillera towards south-east Europe. Eastward the Sakarya zone of northern Turkey is also characterised by Variscan intrusives of similar ages (e.g. Kazdag orthogneiss, zircon $^{207}Pb/^{206}Pb$ step age of 308 ± 16 Ma, OKAY et al., 1996).

This study has shown that crystallization ages (U-Pb on zircon) of Pelagonian basement granitoids range between 308 and 319 Ma. As can be expected from the lower closure temperature, Ar-Ar muscovite ages are 22 to 11 Ma younger than the zircon ages. Petrographic study on mylonitic gneisses and mica schists show syn-deformational crystallization for their mica. Together with the geochronological data this confirms a tectonometamorphic event under Barrovian conditions in late Variscan time, most likely related to the emplacement of the intrusive bodies. The presence of variably deformed magmatic rocks leads to several interpretations for this Late Carboniferous event:
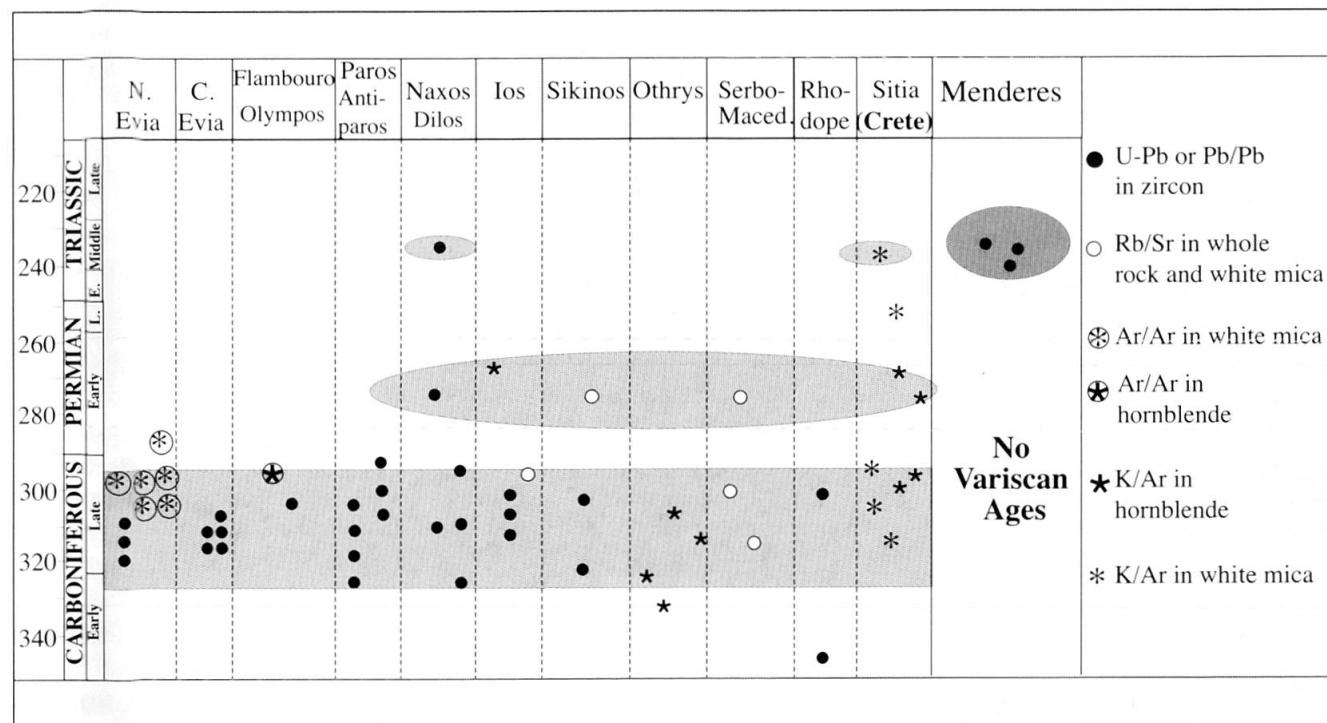
Fig. 9 Compilation of Late Paleozoic-Early Mesozoic absolute ages from the Pelagonia, Cyclades, Rhodope and Menderes basement. References in text. Time scale from GRADSTEIN and OGG (1996).
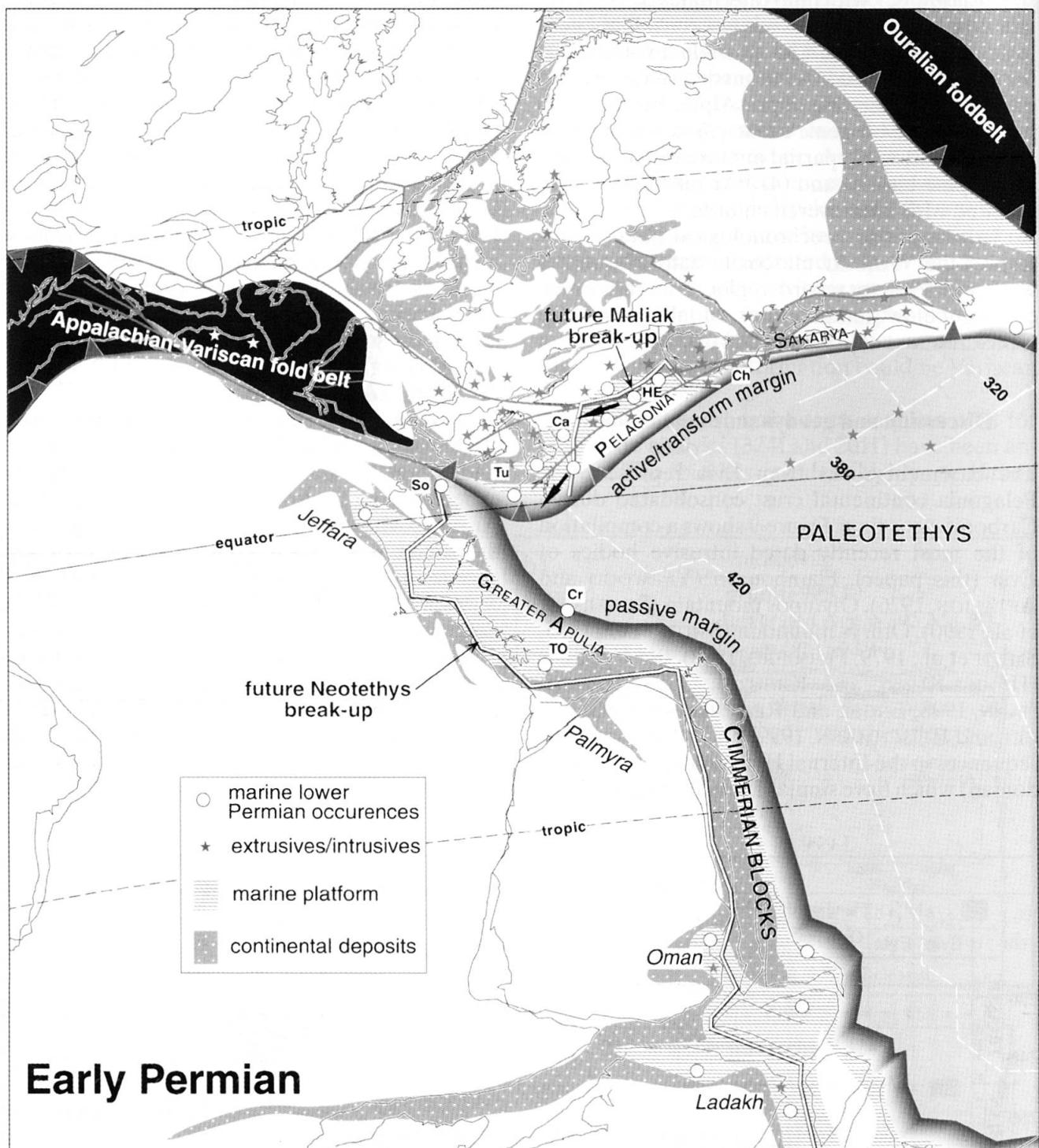
Fig. 10   Early Permian reconstruction of the western Tethyan realm. (Modified from STAMPFLI et al., in press). Ca: Carnic Alps; Ch: Chios; Cr: Late Carboniferous-Permian pelagic sequences from Eastern and Western Crete (Tripali); HE: marine Permian formation from Hydra and Evia; So: Flysch and pelagic Permian sequences from the Sicanian basin of Sicily; TO: Early Permian platform from the Talea Ori group, Crete; Tu: Tuscan Alps.

– The less deformed granitoids were emplaced at 319 and 308 Ma, just after deformation (and perhaps peak of metamorphism) and formation of mylonites in a compressional setting. Following decompression and uplift, the whole sequence comprising metasediments and older intrusive

rocks experienced cooling during Early Permian times.

– Late Carboniferous lithospheric attenuation and decompression of a thickened crust triggered the intrusion of granitoids. This was accompanied by widespread upper greenschist facies metamor-
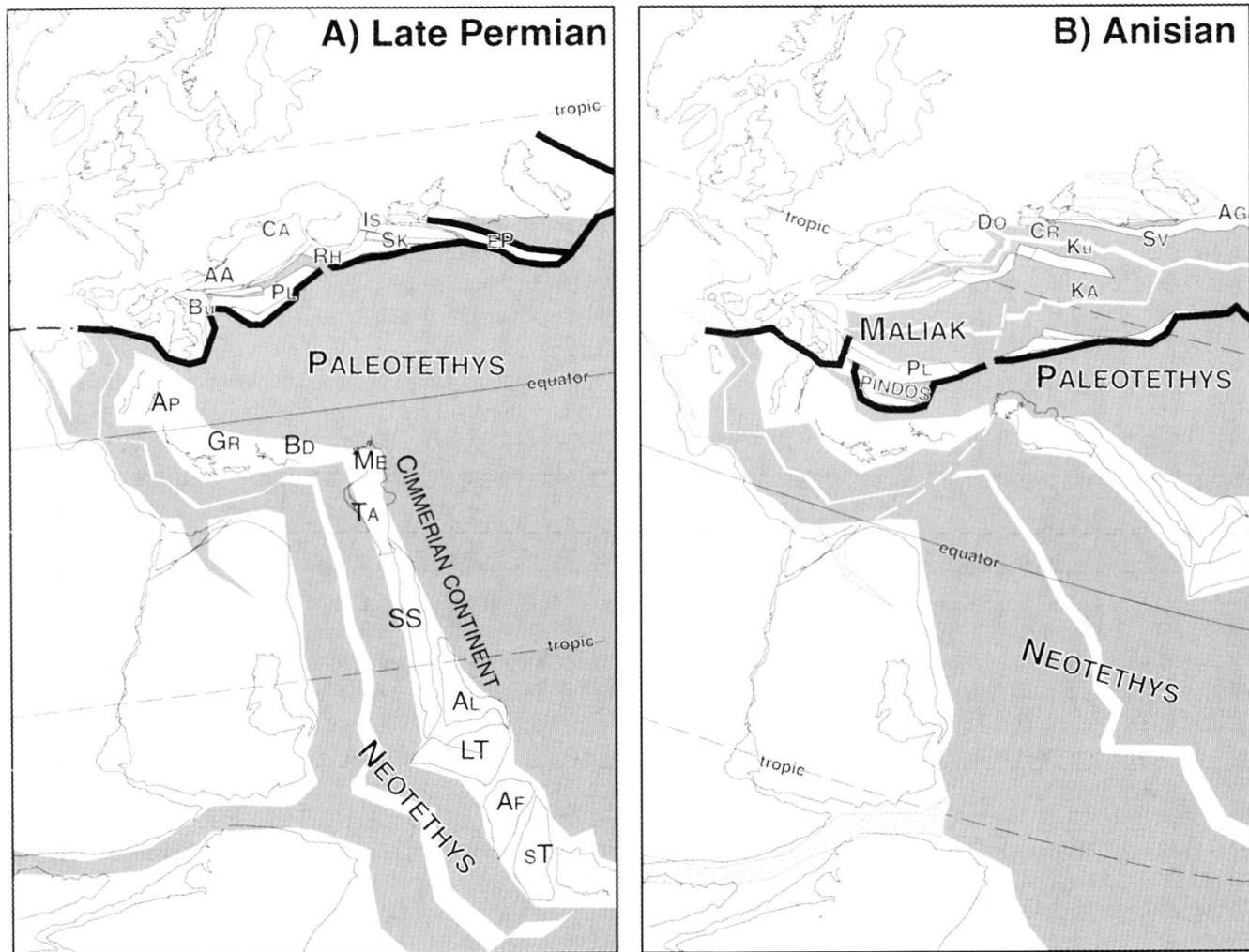
Fig. 11   Late Permian-Middle Triassic reconstruction of the Tethyan realm. (Modified from STAMPFLI et al., in press):
Cimmerian blocks: AF: central Afghanistan; AL: Alborz; AP: Apulia; BD: Bey-Daglari; GR: autochthonous of Greece;
LT: Lut-Tabas; ME: Menderes; SS: Sanandaj-Sirjan; sT: south Tibet; TA: Taurus.
Eurasia: AA: Austro-Alpine; AG: Agh-Darband; BÜ: Bükk; CA: Carpathian; CR: Crimea; DO: Dobrogea; EP: east Pontides; IS: Istanbul; KA: Karakaya, KÜ: Küre; RH: Rhodope; SK: Sakarya; SV: Svanetia; PL: Pelagonia.

phism and activation of crustal scale ductile shear zones.

Two geodynamic models can be proposed: a subduction-related plutonic arc model for the southern Late Carboniferous Variscan orogen (ZIEGLER, 1984; FINGER and STEYER, 1990; STAMPFLI and MOSAR, 1996), as opposed to a Carboniferous to Early Permian intracontinental subduction and collision model as proposed by MATTE (1991) for continental Europe; a solution which could be envisaged in view of the presence of I-type granitoids of calc-alkaline affinity of the Pelagonian basement in continental Greece (KATERINOPOULOS and MARCOPOULOS, 1987); however ENGEL and REISCHMANN (1999) suggested a S-type composition for gneisses of similar age from the Cycladic islands.

We prefer a Late Variscan geodynamic setting of Cordillera-type for the Pelagonian domain in a context of oblique Carboniferous subduction of the Paleotethys, included its mid-ocean ridge and followed by slab detachment. This situation would have evolved in a widespread Permian "Basin and Range" type (KEAREY and VINE, 1996) extensional event, affecting not only this cordillera, but the entire European Variscan orogen. This event, was accompanied by large scale strike slip movements due to the final docking of Gondwana with Laurasia.

This Permo-Carboniferous extension eventually resulted in the opening of back arc basins since Early Permian time along the margin (Maliak, Meliata, Küre, Karakaya... Fig. 10 and 11). Elsewhere in Europe, tectonic collapse of the Variscan orogen, between the Late Carboniferous and the Early Permian, resulted in the development of small intra-continental rifts (Fig. 10). The subduction of the mid-oceanic ridge and/or the

detachment of the Paleotethys oceanic slab caused substantial heating which could be responsible for the emplacement of syn- to post-orogenic granitoids in the Variscan domain in Carboniferous times (BONIN et al., 1998). For example, the Mont-Blanc and central Aar granites dated at 303 Ma by BUSSY and VON RAUMER (1993) and 298 Ma by SCHALTEGGER (1994), respectively, have a geochemistry and zircon typology of alkali-calcic affinity. Other Late Carboniferous to Early Permian granitoids from the Alpine domain display the same characteristics (SCHALTEGGER and GEBAUER, 1999; SCHALTEGGER and CORFU, 1992). Most of these granites often grade into within plate syn-rift, mostly rhyolitic effusives in Early Permian time (SCHALTEGGER, 1994); most of these rifts aborted in Late Permian times.

Large scale strike-slip movements and widespread rifting in the Variscan domain, imply the presence of a free border or active margin located southward of the orogen and not a complete closure of the Paleotethyan domain in Permian time (Fig. 10). Subduction related high Mg-K calc-alkaline plutons, containing stocks or enclaves of melanocratic rocks, have been interpreted as syntectonic pulses of subduction enriched magma and crustal contaminated magma, strongly linked to strike-slip faults. The ages of these granites are between 345 and 330 Ma in the Alpine domain for example (SCHALTEGGER and CORFU, 1992; BUSSY et al., 1998), but can be as young as 310 Ma. The older ages show that subduction of Paleotethys already started during the Early Carboniferous and the arc migrated southward in time.

The idea that the Paleotethys remained open south of the Alpine Variscides until the Early Triassic, is supported by the presence of Early to Late Permian pelagic sediments in the Sicannian basin in Sicily (CATALANO et al., 1988; CATALANO et al., 1995) (So, in Fig. 10) and a complete Late Carboniferous to Early Triassic pelagic sequence found in western (KRAHL et al., 1983) and eastern Crete (Cr, in Fig. 10) (KRAHL et al., 1986), where they are overthrusted by the Variscan Sitia basement. These two occurences belong to the southern Paleotethys passive margin. Besides these, continental to marine Late Carboniferous to Early Permian occurences are found around the arc of the Eurasian active margin, for example in:

– the Tuscan Alps (GATTIGLIO et al., 1989), and south Apennines (Mte Amiata)

– the deep-water Kungurian to Roadian flysch of the clastic Trogkofel beds of RAMOVS (1968) found just south of the Periadriatic line (e.g. KOZUR and MOSTLER, 1992; KOZUR, 1999)

– deep marine clastic sequences of the Carnic and Karawanken Alps (Ca, in Fig. 10).

The Cimmerian unconformity in Crete can be placed between the Early Triassic and the Norian according to KRAHL et al. (1988), and it corresponds to the instalment of a carbonate platform over the deep water deformed sediments of the Paleotethyan accretionary prism such as:

– the Arna unit, with ultramafites and Variscan orthogneiss blocks (PAPANIKOLAOU, 1981; SKARPELIS, 1982; PAPANIKOLAOU, 1984; DANAMOS, 1992)

– part of the Tyros beds, where pelagic Permian is followed by Triassic arc volcanites (KTENAS, 1924; DANAMOS, 1990).

The concomitant Permian opening of the East Mediterranean basin (STAMPFLI et al., 1991; STAMPFLI and PILLEVUIT, 1993; STAMPFLI et al., in press) between Gondwana and the western Cimmerian blocks (Ap, Gr & Bd, in Fig. 11A, i.e: Apulia, external Hellenides and western Taurides) implies the subsequent closure of Paleotethys along a Hellenic transect during the Permian. This Cimmerian orogenic event was accompanied by the emplacement of a few granitoids in Greece (Naxos, Kastoria and Crete) and in the Menderes massif in western Turkey (ME, in Fig. 11A) (DANNAT and REISCHMANN, 1998), dated from Early to Middle Triassic.

In that context, the Pindos basin of Greece (Fig. 11B) with its pelagic sequence starting with a Middle to Late Triassic flysch sequence (FLEURY, 1980) could be regarded as a remnant of a fore-arc basin (PE-PIPER and KOTOPOULI, 1991) also represented by Late Permian (?) to Late Triassic wildflysch of the Liri unit originating from the most external Pelagonian domain (STAMPFLI et al., 1995; STAMPFLI, 1996; DE BONO et al., 1999) in which blocks and pebbles of Late Carboniferous granites are recycled.

Eastward, the suture of Paleotethys in Turkey is represented by the Karakaya mélanges (SENGÖR et al., 1980; OKAY and MOSTLER, 1994 and OKAY et al., 1996) where Paleotethyan material is actually re-cycled in a younger Triassic wildflysch related to the closure of a back-arc rather than the major Paleotethyan ocean (Fig. 11B).

Concerning the dubious Cretaceous ages obtained from the biotites of northern Evia it should be noted that other late Early to Late Cretaceous geochronological ages (120-65 Ma) on white mica, biotite and hornblende have been found in the Pelagonian s.s. realm, such as Othrys (SMITH et al., 1975), Flambouron (MERCIER, 1968; YARWOOD and DIXON, 1977) and Olympos (BARTON, 1976; YARWOOD and DIXON, 1977; SCHERMER et al., 1990), as well as in the Cyclades (Ios) (ANDRIESEN

et al., 1987) and Asteroussia mountains (Crete) (LIPPOLT and BARANYI, 1976; SEIDEL et al., 1976). These data suggest a Cretaceous metamorphic event in the Hellenides.

A well constrained Early Cretaceous metamorphic phase is known in the Rhodope and on Thassos (WAWRZENITZ and MPOSKOS, 1997) and also in the Intra-Pontides suture of NW Turkey (e.g. OKAY et al., 1996). This orogenic phase created the Balkanide mountain belt in late Early Cretaceous (e.g. GEORGIEV et al., 1997), but should not have affected units more external than the Circum-Rhodope/Vardar zone regions, as a remnant Vardar ocean separated both areas at that time. The subduction of this Vardar ocean generated HP ages from Late Cretaceous to Eocene (BRÖCKER and ENDERS, 1999), affecting the Pelagonian and Vardar zone.

Older Mid- to Late Cretaceous ages may correspond to re-heating during this time because of rifting processes in the flexured Pelagonian subducting plate (BONNEAU, 1984). Older Early Cretaceous ages (125–115 Ma) should be related to the obduction of the Vardar ophiolites (BARTON, 1976; YARWOOD and DIXON, 1977) and the detachment of the Maliak ocean slab whereas initial intra-oceanic shearing of these ophiolites has been dated as Middle to Late Jurassic (SPRAY et al., 1984). Obviously, more data are needed to test the significance of these Cretaceous ages.

Conclusions

Analysis of the available pre-Alpine geochronological data from the Pelagonian basement shows that three main tectonometamorphic and magmatic events can be traced through the Carboniferous to Middle Triassic period (Fig. 9):

– Event 1 is well constrained in Evia, Cyclades, Othrys and Crete, ranging in age from late Early Carboniferous to Early Permian. It is considered as related to the Variscan magmatic activity at that time accompanying the northward subduction of Paleotethys (Fig.10) in a context of collision of Gondwana with Laurasia.

– Event 2 corresponds to poorly constrained late Early Permian magmatic activity, traces of which are found in the Cyclades and in Crete. Subduction of Paleotethys slowed down and slab roll-back started to be the dominant geodynamic factor accompanied by the collapse of the Variscan cordillera.

– Event 3 is only recognised in a few places in Greece and Turkey; it represents the final stage of subduction and closure of Paleotethys. This was concomitant with or followed by the detachment

of the oceanic Paleotethyan slab and final collapse of the outer board of the Variscan cordillera (e.g. Pelagonian and Sitia basements). This gave rise to a large scale mid-Triassic volcanic event (Pietra Verde) from northern Italy to western Turkey (Fig. 11B).

The second and third magmatic events are poorly constrained by available data (U/Pb ages of 275 Ma and 233 Ma from the Naxos gneisses reported by REISCHMANN, 1998).

According to STAMPFLI (1996), the European Variscan belt was an active Andean-type margin during Carboniferous-Early Permian times, the Paleotethys oceanic crust being subducted northwards beneath the southern margin of the European continent (Fig. 10). This subduction is considered responsible for the Late Carboniferous to Permian calc-alkaline intrusions found everywhere in the South Alpine and South European Variscan terrains. The widespread Variscan Early Carboniferous magmatic and metamorphic event is directly related to the subduction of the Paleotethys mid-ocean ridge followed by the roll-back of the remnant southern half of Paleotethys and the detachment of its slab accompanied by the collapse of the Variscan cordillera. This led to the Late Permian opening of the Maliak and associated back-arc oceans (Fig. 11A), the syn-rift sequence of which started in Early Permian and characterizes the Pelagonian northern margin (e.g. Hydra island, BAUD et al., 1990 and GRANT et al., 1991; Evia island, DE BONO, 1999 and VAVASSIS, 2000).

The Variscan overprint, characteristic of the Pelagonian basement, was not recorded on the Menderes massif Pan-African basement in western Turkey (SENGÖR, 1984; HETZEL and REISCHMANN, 1996; REISCHMANN, 1998). For this reason the Menderes massif cannot be considered as the eastern continuation of the Attica-Cyclades Massif, as proposed by DÜRR (1986) and JACOBSHAGEN (1986). The Menderes Massif is part of the Cimmerian continents detached from Gondwana by the Permian opening of Neotethys.

the Swiss National Science Foundation (n. 20-39494.93). The major and trace elements chemical analyses were obtained at the Centre d'analyse minérale (University of Lausanne) and the rare earth elements analyses at the XRAL Laboratories (Don Mills, Ontario, Canada). The U-Pb analyses were made at the Royal Ontario Museum. The Ar-Ar analyses were carried out at the Laboratoire des Isotopes of the University of Lausanne.

References

ALTHERR, R., KREUZER, H., WENDT, I., LENZ, H., WAGNER, G.A., KELLER, J., HARRE, W. and HÖHNDORF, A. (1982): A Late Oligocene/Early Miocene High Temperature Belt in the Attic-Cycladic Crystalline Complex (SE Pelagonian,Greece). Geol. Jb. E 23, 97–164.

ANDRIESEN, P.A.M., BANGA, G. and HEBEDA, E.H. (1987): Isotopic age study of pre-Alpine rocks in the basal units on Naxos, Sikinos and Ios, Greek Cyclades. Geologie en Mijnbouw 66, 3–14.

BARTON, C.M. (1976): The tectonic vector and emplacement age of an allochtonous basement slice in the Olympos area, N.E. Greece. Bull. Soc. Geol. France 18, 252–258.

BAUD, A., JENNY, C., PAPANIKOLAOU, D., SIDERIS, C. and STAMPFLI, G.M. (1990): New observations on the Permian stratigraphy in Greece and geodynamic interpretation. In: 5th. Cong. Geol. Soc. of Greece, Thessaloniki. Bull. Geol. Soc. of Greece XXV/1, 187–206.

BAUMGARTNER, P.O. and BERNOULLI, D. (1976): Stratigraphy and Radiolarian Fauna in a Late Jurassic-Early Cretaceous Section near Achladi (Evvoia, Eastern Greece). Eclog. geol. Helv. 69, 601–626.

BENISCHEK, A. and FINGER, F. (1993): Factors controlling the development of prism faces in granite zircons: a microprobe study. Contr. Mineral. Petrol. 114, 441–451.

BONIN, B., AZZOUNI-SEKKAL, A., BUSSY, F. and FERRAG, S. (1998): Alkali-calcic to alkaline post-collision granite magmatism: petrologic constraints and geodynamic settings. Lithos 45, 45–70.

BONNEAU, M. (1984): Correlation of the Hellenide nappes in South-east Aegean and their tectonic reconstruction. In: DIXON, J.E. and ROBERTSON, A.H.F. (eds): The Geological Evolution of the Eastern Mediterranean. Spec. Publ. Geol. Soc. London 17, 517–527.

BORSI, S., FERRARA, G. and MERCIER, J. (1966): Mesures d'âge par la méthode Rb/Sr des granites filoniens de Karathodoro (zones internes des Hellénides, Macédoine centrale, Grèce). Savez Geol. Drus. Szr. Jugoslavije, 5–10.

BRÖCKER, M. and FRANZ, L. (1998): Rb-Sr isotope studies on Tinos Island (Cyclades, Greece): additional time constraints for metamorphism, extent of infiltration-controlled overprinting and deformational activity. Geol. Mag. 135, 369–382.

BRÖCKER, M. and ENDERS, M. (1999): U-Pb zircon geochronology of unusual eclogite-facies rocks from Syros and Tinos (Cyclades, Greece). Geol. Mag. 136, 111–118.

BUSSY, F. and VON RAUMER, J. (1993): U-Pb dating of Paleozoic events in the Mont Blanc crystalline massif, Western Alps. Terra abstracts 5, 382–383.

BUSSY, F., DÉLITROZ, D., FELLAY, R. and HERNANDEZ, J. (1998): The Pormenaz monzonite (Aiguilles Rouges, western Alps): an additional evidence for a 330 Ma-

old magnesiopotassic magmatic suite in the Variscan Alps. Schweiz. Mineral. Petrogr. Mitt. 78, 193–194.

CATALANO, R., DISTEFANO, P. and KOZUR, H. (1988): New results in the Permian and Triassic stratigraphy of western Sicily with special reference to the section at Torrente San Calogero, SW of Pietra di Salome (Sosio valley). Soc. geol. Italiana. Atti del 74 Congresso Nazionale, A, 119–125.

CATALANO, R., DI STEFANO, P. and VITALE, F.P. (1995): Structural trends and paleogeography of the central and western Sicily belts: new insight. Terra Nova 7, 189–199.

CELET, P. and FERRIÈRE, J. (1978): Les Hellénides internes: Le Pélagonien. Eclogae geol. Helv. 71, 467–495.

COSCA, M.A., METZGER, K. and ESSENE, E.J. (1998): The Baltica-Laurentia Connection: Sveconorwegian (Grenvillan) Metamorphism, Cooling and Unroofing in the Bable Sector, Norway. J. Geol. 106, 539–552.

DANAMOS, G. (1990): The presence of "Tyros beds" formation at Kythira island. In: 5th Congress of the Geological Society of Greece, Thessaloniki. Bull. Geol. Soc. Greece XXV/1, 399–404.

DANAMOS, G. (1992): Contribution to geology and hydrogeology of the Island of Kythira. Ph.D. Thesis, Athens.

DANNAT, C. and REISCHMANN, T. (1998): Geochronological, geochemical and isotopic data on granitic gneisses from the Menderes Massif, SW Turkey. In: Third International Turkish Geology Symposium, Ankara. Abstracts volume, 282.

DANNAT, C. and REISCHMANN, T. (1999): Single zircon ages of migmatites from the Menderes Massif, SW Turkey. In: EUG 10, Strasbourg. Abstract volume, 805.

DE BONO, A. (1998): Pelagonian margins in central Evia island (Greece). Stratigraphy and geodynamic evolution. Ph.D. Thesis, University of Lausanne, 114 pp.

DE BONO, A., VAVASSIS, I., STAMPFLI, G.M., MARTINI, R., VACHARD, D. and ZANINETTI, L. (1999): New stratigraphic data on the Pelagonian pre-Jurassic units of Evia island, (Greece). Ann. Géol. Pays Hellén. 38, 11–24.

DÜRR, S. (1986): Das Attisch-kykladische Kristallin. In: JACOBSHAGEN (ed.): Geologie von Griechenland. 116–149.

DÜRR, S. and FLÜGEL, E. (1979): Contribution à la stratigraphie du cristallin des Cyclades: mise en évidence de Trias supérieur dans les marbres de Naxos (Grèce). Rapp. Comm. Intern. Mer. Médit. 25/26, 31–31.

ENGEL, M. and REISCHMANN, T. (1998): Single Zircon geochronology of orthogneisses from Paros, Greece. In: 8th Intern. Congr. of the Geol. Soc. of Greece, Patras. Bull. Geol. Soc. of Greece XXXII/3, 91–99.

ENGEL, M. and REISCHMANN, T. (1999): Geochronology of the Pre-Alpine Basement in the Central Cyclades, Greece. EUG 10, Strasbourg. Abstract volume, 806.

FERRIÈRE, J. (1982): Paléogéographie et tectoniques superposées dans les Hellénides internes: le massifs de l'Othrys et du Pelion (Grèce continentale). Soc. géol. Nord Publ. 8–1, 1–493.

FINGER, F. and STEYER, H.P. (1990): I-type granitoids as indicators of a late Paleozoic convergent ocean continent margin along the southern flank of the central European Variscan orogen. Geology 18, 1207–1220.

FLEURY, J.J. (1980): Les Zones de Gavrovo Tripolitza et du Pinde-Olonos (Grèce continentale et Pélopon-

nèse du Nord). Evolution d'une plate-forme et d'un bassin dans leur cadre alpin. Soc. Géol. Nord. Publ. 4, I, 9–473.

GATTIGLIO, M., MECCHERI, M. and TONGIORGI, M. (1989): Stratigraphic correlation forms of the Tuscan Paleozoic basement. In: SASSI, F.P. and ZANFERRARI, A. (eds): Pre-Variscan and Variscan events in the Alpine-Mediterranean belts, Stratigraphic correlation forms. Rend. Soc. geol. Ital., Roma, 245–257.

GRADSTEIN, F.M. and OGG, J.G. (1996): A Phanerozoic time scale. Episodes 19.

GRANT, R.E., NESTELL, M.K., BAUD, A. and JENNY, C. (1991): Permian Stratigraphy of Hydra Island, Greece. Palaios 6, 479–497.

GUERNET, C. (1975): Sur l'existence en Eubée moyenne d'une nappe constituée principalement de roches vertes et de leur couverture mésozoique. Extr. Ann. Soc. géol. du Nord XCV, 59–66.

HASKIN, L.A., HASKIN, M.A., FREY, F.A. and WILDMAN, T.R. (1968): Relative and absolute terrestrial abundances of the rare earths. In: AHRENS, L.H. (ed.): Origin and distribution of the elements. Pergamon, Oxford, 889–911.

HENJES-KUNST, F. and KREUZER, H. (1982): Isotopic Dating of Pre-Alpidic Rocks from the Island of Ios (Cyclades, Greece). Contr. Mineral. Petrol. 80, 245–253.

HETZEL, R. and REISCHMANN, T. (1996): Intrusion age of Pan-African augengneisses in the southern Menderes massif and age of cooling after Alpine ductile extensional deformation. Geol. Mag. 133, 565–572.

HETZEL, R., ROMER, R.L., CANDAN, O. and PASCHIER, C.W. (1998): Geology of the Bozdag area, central Menderes massif, SW Turkey: Pan-African basement and Alpine deformation. Geol. Rundsch. 87, 394–406.

JACOBSHAGEN, V. (1986): Geologie von Griechenland. Gebrüder Borntraeger, Berlin, 363.

JACOBSHAGEN, V. and ROEDER, D. (1976): Die eohellenische Phase, Definition und Interpretation. Z. dtsch. geol. Ges. 127, 133–145.

KATERINOPOULOS, A. and MARCOPOULOS, T. (1987): Acid magmatism in the Pelagonian and Rhodope belts (Macedonia-Greece). In: FLÜGEL, H.W., SASSI, F.P. and GRECULA, P. (eds): Pre-Variscan and Variscan events in the Alpine-Mediterranean mountain belts. Mineralia Slovaca, Alfa Bratislava, 323–328.

KATSIKATSOS, G. (1977a): L'Eubée meridionale / L'Eubée centrale. Bull. Soc. géol. France XIX, 105–110.

KATSIKATSOS, G. (1977b): La structure tectonique de l'Attique et de l'île Eubée. Bull. Soc. géol. France XIX, 75–80.

KATSIKATSOS, G. (1992): The geology of Greece. Athens, 451 pp.

KATSIKATSOS, G., MIGIROS, G. and VIDAKIS, M. (1980): Remarks on the geology of the area between Mavrouni and Olympus (Greece). 26e Congrès Géologique International, Paris III, 1391.

KATSIKATSOS, G., MIGIROS, G., TRIANTAPHYLLIS, M. and METTOS, A. (1986): Geological structure of the internal Hellenides (E. Thessaly-SW. Macedonia, Euboea-Attica-Northern Cyclades Islands and Lesvos). Athens, 191–212.

KEAREY, P. and VINE, F.J. (1996): Global Tectonics. Blackwell Science, 333pp.

KIRSCHNER, D.L., COSCA, M.A., MASSON, H. and HUNZIKER, J.C. (1996): Staircase $^{40}Ar/^{39}Ar$ spectra of fine-grained white mica: Timing and duration of de-

formation and empirical constraints on argon diffusion. Geology 24, 747–750.

KOKKINAKIS, A. (1978): Das Intrusivgebiet des Synvolon-Gebirges und von Kavalla in Ostmakedonien, Griechenland. Dr. Thesis, Univ. München, 255 pp.

KOZUR, H.W. (1999): Permian development in the western Tethys. In: Shallow Tethys 5, Chiang Mai, 101–135.

KOZUR, H. and MOSTLER, H. (1992): Erster paläontologischer Nachweis von Meliaticum und Süd-Rudabànyaicum in den nördlichen Kalkalpen (Oesterreich) und ihre Beziehungen zu den Abfolgen in den Westkarpaten. Geol. Paläont. Mitt. Innsbruck 18, 87–129.

KRAHL, J., KAUFFMANN, G., KOZUR, H., RICHTER, D., FÖRSTER, O. and HEINRITZI, F. (1983): Neue Daten zur Biostratigraphie und zur tektonischen Lagerung der Phyllit-Gruppe und der Trypali-Gruppe auf der Insel Kreta (Griechenland). Geol. Rundsch. 72, 1147–1166.

KRAHL, J., KAUFFMANN, G., RICHTER, D., KOZUR, H., MÖLLER, I., FÖRSTER, O., HEINRITZI, F. and DORNSIEPEN, U. (1986): Neue Fossilfunde in der Phyllit-Gruppe Ostkretas (Griechenland). Z. dt. geol. Ges. 137, 523–536.

KRAHL, J., RICHTER, D., FÖRSTER, O., KOZUR, H. and HALL, R. (1988): Zur Stellung der Talea Ori im Bau des kretischen Deckenstapels (Griechenland). Z. dtsch. geol. Ges. 139, 191–227.

KRAMAR, N., COSCA, M. and HUNZIKER, J. (1998): Simple shear deformation and argon retention in muscovite: Insights from UV-laser ablation $^{40}Ar/^{39}Ar$ ages of pegmatitic white mica of the Siviez-Mischabel nappe (western Swiss Alps). In: American Geophysical Union Fall Meeting, San Francisco. EOS, Transactions 79, 955.

KROGH, T.E (1973): A low-contamination method for hydrothermal decomposition of zircon and extraction of U and Pb for isotopic age determinations. Geochim. Cosmochim. Acta, 37, 485–494.

KROGH, T.E (1982): Improved accuracy of U-Pb zircon ages by the creation of more concordant system using an air abrasion technique. Geochim. Cosmochim. Acta, 46, 637–649.

KTENAS, C. (1924): Formations primaires semimétamorphiques au Péloponnèse central. C. R. somm. Soc. Géol. France 24, 61–63.

LIPPOLT, H.J. and BARANYI, I. (1976): Oberktretazische Biotit und Gesteinsalter aus Kreta. N. Jb. Geol. Pal.Mh. H. 7, 404–414.

LISTER, G.S., BALDWIN, S.L., RAOUZAIOS, A. and VANDENBERG, L.C. (1994): Magmas, metamorphism and deformation during the tectonic evolution of the Aegean sea. In: 12th Australian Geological Convention, Perth, 250–251.

MATTE, P. (1991): Accretionary history and crustal evolution of the Variscan belt in western Europe. Tectonophysics 196, 309–337.

MELIDONIS, N.G. (1980): The geological structure and mineral deposits of Tinos Island (Cyclades, Greece). The geology of Greece 13, 1–80.

MERCIER, J. (1968): Etude géologique des zones internes des Hellénides en Macédoine centrale (Grèce). Ann. géol. Pays Hellén. 20, 1–792.

MOUNTRAKIS, D. (1986): The Pelagonian zone in Greece: a polyphase-deformed fragment of the Cimmerian Continent and its role in the geotectonic evolution of the Eastern Mediterranean. J. Geol. 94, 335–347.

NAKAMURA, N. (1974): Determination of REE, Ba, Mg,

Na and K in carbonaceous and ordinary chondrites. Geochim. Cosmochim. Acta 38, 757–775.

NEGRIS, P.K. (1915): Roches cristallophylliennes et tectonique de la Grèce. Athènes, 123.

OKAY, A.I. and MOSTLER, H. (1994): Carboniferous and Permian Radiolarite Blocks from the Karakaya Complex in Northwest Turkey. Turkish J. Earth Sci. 3, 23–28.

OKAY, A.I., SATIR, M., MALUSKI, H., SIYAKO, M., MONIE, P., METZGER, R. and AKYÜZ, S. (1996): Paleo- and Neo-Tethyan events in northwestern Turkey: geologic and geochronologic constraints. In: YIN, A. and HARRISON, T.M. (eds): The tectonic evolution of Asia. Cambridge University Press, 420–441.

PAMIC, J., LANPHER, M. and BELAK, M. (1996): Hercynian I-type and S-type granitoids from the Slavonian mountains (southern Pannonian Basin, northern Croatia). N. Jb. Miner. Abh. 1782, 155–186.

PAPANIKOLAOU, D. (1978): Contribution to the Geology of the Aegean Sea : The Island of Andros. Ann. Géol. Pays Hellén. 29/2, 477–553.

PAPANIKOLAOU, D. (1979): Unités tectoniques et phases de déformation dans l'île de Samos, Mer Egée, Grèce. Bull. Soc. Géol. France XXI, 745–752.

PAPANIKOLAOU, D. (1980): Contribution to the geology of Aegean Sea: The Island of Paros. Ann. Géol. Pays Héllen. 30/1, 65–96.

PAPANIKOLAOU, D. (1981): Remarks on the kinematic interpretation of folds from some cases of the Western Swiss Alps and of the Hellenides. Ann. Géol. Pays Hellén. 30, 741–762.

PAPANIKOLAOU, D. (1984): The three metamorphic belts of the Hellenides: a review and a kinematic interpretation. Spec. Publ. Geol. Soc. London. 17, 551–561.

PAPANIKOLAOU, D. (1989): Are the medial Crystalline massifs of the Eastern Mediterranean drifted Godwanian fragments? Spec. Public. Geol. Soc. Greece 1, 63–90.

PAPANIKOLAOU, D. and ZAMBETAKIS-LEKKAS, A. (1980): Nouvelles observations et datations de la base de la serie pélagonienne (s.s.) dans la région de Kastoria, Grèce. C.R. Acad. Sc.Paris 291, 155–158.

PAPANIKOLAOU, D. and SASSI, F.P. (1989): Paleozoic Geodynamic domains and their alpidic evolutions in the Tethys. Spec. Public. Geol. Soc. Greece 1, 7–10.

PARROT, J.F. and GUERNET, C. (1972): Le cortège ophiolitique de l' Eubée moyenne (Grèce): étude pétrographique des formations volcaniques et des roches métamorphiques associées dans les Monts Kandilis aux radiolarites. Cah. ORSTOM, ser. Géol. IV, 153–161.

PE-PIPER, G. and KOTOPOULI, C.N. (1991): Geochemical characteristics of the Triassic igneous rocks of the island of Samos, Greece. N. Jb. Mineral. Abh. 162, 135–150.

PE-PIPER, G. and KOTOPOULI, N. (1997): Geochemistry of metamorphosed mafic rocks from Naxos (Greece): The Cenozoic history of the Cycladic crystalline belt. Ofioliti 22, 239–249.

PE-PIPER, G., DOUTSOS, T. and MPORONKAY, C. (1993): Structure, geochemistry and mineralogy of Hercynian granitoid rocks of the Verdikoussa area, Northern Thessaly, Greece and their regional significance. N. Jb. Mineral. Abh. 165, 267–296.

PEARCE, J.A. (1982): Trace element characteristics of lavas from destructive plate boundaries. In: THORPE, R.S. (ed.): Andesites. John Wiley & Sons, 525–548.

PEARCE, J.A., HARRIS, N.B.W and TINDLE, A.G. (1984): Trace element discrimination diagrams for the tectonic interpretation of the granitic rocks. J. Petrol. 25, 956–983.

PUPIN, J.P. (1976): Signification des caractères morphologiques du zircon commun des roches en pétrologie. Base de méthode typologique. Applications. Thèse d'Etat Univ. Nice (France), 394 pp.

PUPIN, J.P. (1978): Rôle de l'eau sur les caractères morphologiques et la cristallisation du zircon dans les granits. Bull. Soc. Géol. Fr. XX, 721–725.

PUPIN, J.P. (1980): Zircon and granite petrology. Contrib. Mineral. Petrol. 73, 207–220.

PUPIN, J.P. (1988): Granites as indicators in paleogeodynamics. Rend. Soc. Ital. Mineral. Petrol. 43, 237–262.

PUPIN, J.P. and TURCO, G. (1972): Le zircon accessoire en géothermométrie. C.R. Acad. Sci. Paris 274, 2121–2124.

RAMOVS, A. (1968): Biostratigraphie der kretischen Entwicklung der Trogkofelstufe in den Karawanken und Nachbargebieten. N. Jb. Geol. Paläont. Abh. 131, 72–77.

REISCHMANN, T. (1998): Pre-Alpine origin of tectonic units from the metamorphic complex of Naxos, Greece, identified by single zircon Pb/Pb dating. In: 8th Intern. Congr. Geol. Soc. Greece, Patras, Greece. Bull. Geol. Soc. Greece XXXII/3, 101–111.

RENZ, C. (1955): Die vorneogene Stratigraphie der normalsedimentären Formationen Griechenlands. No. Inst. Geol. Sub. Res. Athens.

RICHTER, D., MÜLLER, C. and RISCH, H. (1996): Die Flysch-Zonen Griechenlands XI. Neue Daten zur Stratigraphie und Paläogeographie des Flysches und seiner Unterlage in der Pelagonischen Zone (Griechenland). N. Jb. Geol. Paläont. Abh. 201, 327–366.

ROBERTSON, A.H.F. (1990): Late Cretaceous oceanic crust and Early Tertiary foreland basin development, Euboea, Eastern Greece. Terra Nova 2, 333–339.

SAMSON, S.D. and ALEXANDER, E.C. (1987): Calibration of the interlaboratory $^{40}Ar/^{39}Ar$ dating standard MMhb-1. Chem. Geol. 66, 27–34.

SCHALTEGGER, U. (1994): Unraveling the pre-Mesozoic history of Aar and Gotthard massifs (Central Alps) by isotopic dating – review. Schweiz. Mineral. Petrogr. Mitt. 74, 41–51.

SCHALTEGGER, U. and CORFU, F. (1992): The age and source for late Hercynian magmatism in the Central Alps: Evidence from precise U-Pb ages and initial Hf isotopes. Contr. Mineral. Petrol. 111, 329–344.

SCHALTEGGER, U. and GEBAUER, D. (1999): Pre-Alpine geochronology of the Central, Western and Southern Alps. Schweiz. Mineral. Petrogr. Mitt. 79, 79–87.

SCHERMER, E.R., LUX, D.R. and BURCHFIEL, C.B. (1990): Temperature-time history of subducted continental crust, mount Olympos region. Tectonics 9, 1165–1195.

SEIDEL, E., OKRUSCH, M., KREUZER, H., RASCHKA, H. and HARRE, H. (1976): Eo-Alpine Metamorphism in the Uppermost Unit of the Cretan Nappe System – Petrology and Geochronology Part 1. The Lendas Area (Asteroussia Mountains). Contrib. Mineral. Petrol. 57, 259–275.

SEIDEL, E., KREUZER, H. and HARRE, W. (1982): A Late Oligocene/Early Miocene High Pressure Belt in the External Hellenides. Geol. Jb. E 23, 165–206.

SENGÖR, A.M.C. (1984): Timing of tectonic events in the Menderes massif, Western Turkey: implications for tectonic evolution and evidence for Pan-African basement in Turkey. Tectonics 3, 693–707.

SENGÖR, A.M.C., YILMAZ, Y. and KETIN, I. (1980): Remnants of a pre-Late Jurassic ocean in the northern

Turkey: fragments of Permian-Triassic Paleo-Tethys? Geol. Soc. Am. Bull. 91, 599–609.

SIDERIS, C. (1989): Geotectonic position of the Upper Paleozoic in Greece: Evolution of concepts. Geologické prace, Bratislava 88, 191–202.

SKARPELIS, N. (1982): Metallogeny of massive sulfides and petrology of the External Metamorphic Belt of the Hellenides (SE Peloponnesus). Thesis, University of Athens, 149 pp.

SMITH, A.G., HYNES, A.J., MENZIES, M., NISBET, E.G., PRICE, I., WELLAND, J. and FERRIÈRE, J. (1975): The Stratigraphy of the Othris Mountains, Eastern Central Greece: a deformed Mesozoic Continental Margin Sequence. Eclogae geol. Helv. 68/3, 463–481.

SMITH, A.G., WOODCOCK, N.H. and NAYLOR, M.A. (1979): The structural evolution of a Mesozoic continental margin, Othris Mountains, Greece. J. geol. Soc. London 136, 589–603.

SPRAY, J.G., BÉBIEN, J., REX, D.C. and RODDICK, J.C. (1984): Age constraints on the igneous and metamorphic evolution of the Hellenic-Dinaric ophiolites. In: DIXON, J.E. and ROBERTSON, A.H.F. (eds): The Geological Evolution of the Eastern Mediterranean. Spec. Publ. Geol. Soc. London. 17, 619–627.

STAMPFLI, G.M. (1996): The Intra-Alpine terrain: A Paleotethyan remnant in the Alpine Variscides. Eclogae geol. Helv. 89, 13–42.

STAMPFLI, G.M. and PILLEVUIT, A. (1993): An alternative Permo-Triassic reconstruction of the kinematics of the Tethyan realm. In: DERCOURT, J., RICOU, L.E. and VRIELYNCK, B. (eds): Atlas Tethys, Palaeoenvironmental maps, explanatory notes. Gaultier-Villards, Paris, 55–62.

STAMPFLI, G.M. and MOSAR, J. (1996): Paleozoic evolution of the Tethyan domain. In: Comparative evolution of peri-Tethyan rift basins, Cairo. Centennial Geol. Soc. Egypt, 182–184.

STAMPFLI, G., MARCOUX, J. and BAUD, A. (1991): Tethyan margins in space and time. In: Paleogeography and paleoceanography of Tethys. In: CHANNELL, J.E.T., WINTERER, E.L. and JANSA, L.F. (eds): Palaeogeography, Palaeoclimatology, Palaeoecology 87, 373–410.

STAMPFLI, G.M., DE BONO, A. and VAVASSIS, I. (1995): Pelagonian basement and cover in Euboea (Greece). Abstract supplement 1, Terra nova 7, 180.

STAMPFLI, G.M., MOSAR, J., DE BONO, A. and VAVASSIS, I. (1998): Late Paleozoic, Early Mesozoic Plate Tectonics of the Western Tethys. In: 8th Intern. Congr. of the Geol. Soc. of Greece, Patras. Bull. Geol. Soc. of Greece XXXII/1, 113–120.

STAMPFLI, G.M., MOSAR, J., FAVRE, P., PILLEVUIT, A. and VANNAY, J.-C. (in press): Late Paleozoic to Mesozoic evolution of the western Tethyan realm: the Neotethys/East-Mediterranean connection. In: CAVAZZA, W., ROBERTSON, A.H.F. and ZIEGLER, P.A. (eds): Peritethyan rift / wrench basins and passive margins, IGCP 369 Bull. Museum Nat. Hist., Paris.

VAVASSIS, I. (2000): Geology and Tectonic Evolution of the Pelagonian zone in Northern Evia Island, Greece. Constraints and geodynamic implications for the Hellenides. Ph.D. Thesis, University of Lausanne, in press.

VAVRA, G. (1992): Systematics of internal zircon morphology in major Variscan granitoid types. Contrib. Miner. Petrol. 117, 331–344.

VERGELY, P. (1984): Tectonique des ophiolites dans les Hellénides internes. Conséquences sur l'évolution des régions téthysiennes occidentales. Thèse, Univ. Paris Sud, 649 pp.

WAWRZENITZ, N. (1997): Mikrostukturell unterstützte Datierung von Deformationsinkrementen in Myloniten: Dauer der Exhumierung und Aufdomung des metamorphen Kernkomplexes der Insel Thassos (Süd-Rhodope, Nordgriechenland). Dr. Thesis, Friedrich-Alexander-Universität, Erlangen-Nürnberg, 193 pp.

WAWRZENITZ, N. and MPOSKOS, E. (1997): First evidence for Lower Cretaceous HP/HT-Metamorphism in the Eastern Rhodope, north Aegean region, north-east Greece. Eur. J. Mineral. 9, 659–664.

YARWOOD, G.A. and AFTALION, M. (1976): Field relations and U-Pb geochronology of a granite from the Pelagonian zone of the Hellenides (High Pieria, Greece). Bull. Soc. Géol. France XVIII, 259–264.

YARWOOD, G.A. and DIXON, J.E. (1977): Lower Cretaceous and younger thrusting in the Pelagonian Rocks of the High Pieria, Greece. In: VI Coll. Geol. Aegean Region, Athens, Greece. 1, 269–280.

ZIEGLER, P.A. (1984): Caledonian and Hercynian crustal consolidation of western and central Europe – a working hypothesis. Geol. en Mijnb. 63, 93–108.